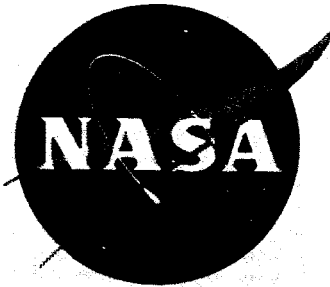


NASA CR-54977

GA-7064



GPO PRICE \$ \_\_\_\_\_

CFSTI PRICE(S) \$ \_\_\_\_\_

Hard copy (HC) 3.00

Microfiche (MF) .25

ff 653 July 65

FACILITY FORM 602

**N66 29477**

(ACCESSION NUMBER)

(THRU)

70

(PAGES)

1

(CODE)

CR-54977

(NASA CR OR TMX OR AD NUMBER)

23

(CATEGORY)

# MEASUREMENT OF NEUTRON SPECTRA IN LIQUID HYDROGEN

by

G. D. Trimble and G. K. Houghton

prepared for

NATIONAL AERONAUTICS AND SPACE ADMINISTRATION

Contract NAS 3-6217

**GENERAL ATOMIC**

A DIVISION OF

**GENERAL DYNAMICS**

JOHN JAY HOPKINS LABORATORY FOR PURE AND APPLIED SCIENCE

P.O. BOX 608 SAN DIEGO 12, CALIFORNIA

## NOTICE

This report was prepared as an account of Government-sponsored work. Neither the United States, nor the National Aeronautics and Space Administration (NASA), nor any person acting on behalf of NASA:

- A.) Makes any warranty or representation, expressed or implied, with respect to the accuracy, completeness, or usefulness of the information contained in this report, or that the use of any information, apparatus, method, or process disclosed in this report may not infringe privately owned rights; or
- B.) Assumes any liabilities with respect to the use of, or for damages resulting from the use of, any information, apparatus, method or process disclosed in this report.

As used above, "person acting on behalf of NASA" includes any employee or contractor of NASA, or employee of such contractor, to the extent that such employee or contractor of NASA, or employee of such contractor, prepares, disseminates, or provides access to, any information pursuant to his employment or contract with NASA, or his employment with such contractor.

Requests for copies of this report should be referred to

National Aeronautics and Space Administration  
Office of Scientific and Technical Information  
Attention: AFSS-A  
Washington, D. C. 20546

**GENERAL ATOMIC**  
DIVISION OF  
**GENERAL DYNAMICS**

JOHN JAY HOPKINS LABORATORY FOR PURE AND APPLIED SCIENCE

P.O. BOX 608, SAN DIEGO, CALIFORNIA 92112

NASA CR-54977  
GA-7064

**MEASUREMENT OF NEUTRON SPECTRA IN LIQUID HYDROGEN**

---

Quarterly Progress Report for the Period Ending March 17, 1966

Work done by:

J. H. Audas  
J. R. Beyster  
J. H. Diaz  
P. L. Heid  
G. K. Houghton  
D. L. Huffman  
D. Mendez  
P. L. Phelps  
A. E. Profio  
J. W. Riggs  
J. C. Sayer  
G. D. Trimble  
J. C. Young

Report written by:

G. D. Trimble  
G. K. Houghton

prepared for  
NATIONAL AERONAUTICS AND SPACE ADMINISTRATION

March 7, 1966

Contract NAS 3-6217

Technical Management  
NASA-Lewis Research Center  
Advanced Development and Evaluation Division  
Nuclear Rocket Technology Office  
John C. Liwosz

## CONTENTS

	<u>Page</u>
1. INTRODUCTION. . . . .	1
2. LIQUID HYDROGEN FACILITY. . . . .	1
2.1 Remote Control Liquid Hydrogen Console . . . . .	2
2.2 Liquid Hydrogen Cryostat and Experimental Facility . . . . .	6
2.2.1 Sheet Metal Enclosure and Work Platform . . . . .	6
2.2.2 Ventilation . . . . .	8
2.2.3 Liquid Hydrogen Cryostat Support System. . . . .	8
2.2.4 Vacuum . . . . .	11
2.2.5 Valve Package. . . . .	11
2.2.6 "Bottle Farm". . . . .	11
2.2.7 Connections from LH <sub>2</sub> Cryostat to Valve Package . . . . .	13
2.2.8 Vacuum Jacketed Transfer Lines from the Valve Package to the LH <sub>2</sub> Supply Dewar . . . . .	13
2.3 Checkout of the Liquid Hydrogen Facility Using Liquid Nitrogen . . . . .	19
3. WATER-COOLED ISOTROPIC FAST NEUTRON SOURCE . . . . .	19
4. FAST NEUTRON SOURCE MONITORS . . . . .	23
5. PROBE TUBE ALIGNMENT MECHANISM . . . . .	25
6. BACKGROUND PLUG USED FOR THE THERMAL NEUTRON SPECTRUM MEASUREMENTS . . . . .	29
7. THEORETICAL CALCULATIONS OF NEUTRON SPECTRA . . . . .	31
7.1 Thermal Neutron Energy Spectrum Calculations . . . . .	31
7.1.1 Energy Levels. . . . .	31
7.1.2 Details of the Calculations. . . . .	31
7.2 Intermediate Neutron Energy Spectrum Calculations. . . . .	34
7.2.1 Energy Levels. . . . .	34
7.2.2 Details of the Calculations. . . . .	46
8. NEUTRON SPECTRUM MEASUREMENTS BY TIME-OF- FLIGHT TECHNIQUES . . . . .	48
8.1 Thermal Neutron Spectrum Measurements . . . . .	48
8.2 Fast Neutron Spectrum Measurements . . . . .	57
8.3 Intermediate Neutron Spectrum Measurements . . . . .	63
9. WORK PLANNED FOR NEXT REPORT PERIOD . . . . .	63
REFERENCES . . . . .	65



## LIST OF FIGURES

<u>Figure</u>		<u>Page</u>
1	Liquid hydrogen console . . . . .	3
2	Sheet metal enclosure showing flexible ducting for intake air supply. . . . .	7
3	Liquid hydrogen support structure. . . . .	10
4	Close-up photograph of valve package . . . . .	12
5	"Bottle farm" area showing the LH <sub>2</sub> supply dewar and helium tube trailer. . . . .	14
6	Revised valve and piping system schematic. . . . .	15
7	Details of the water-cooled 3-in. diameter spherical uranium fast neutron source. . . . .	21
8	Fast neutron spectrum of a 3-in. diameter water-cooled depleted uranium source at an angle of 94° . . . . .	22
9	Aluminum monitor system . . . . .	24
10	Cutaway view of the probe tube alignment system. . . . .	27
11	Photograph of the alignment plate . . . . .	28
12	B <sup>10</sup> background plug . . . . .	30
13	S <sub>4</sub> calculation of the thermal neutron spectra for 2.5 in. of liquid hydrogen . . . . .	35
14	S <sub>4</sub> calculation of the thermal neutron spectra for 4.5 in. of liquid hydrogen . . . . .	36
15	S <sub>4</sub> calculation of the thermal neutron spectra for 7.0 in. of liquid hydrogen . . . . .	37
16	S <sub>4</sub> calculation of the thermal neutron spectra for 10.5 in. of liquid hydrogen . . . . .	38
17	S <sub>4</sub> calculation of the thermal neutron spectra for 13.0 in. of liquid hydrogen . . . . .	39
18	S <sub>8</sub> calculation of the thermal neutron spectra for 2.5 in. of liquid hydrogen at angles of 28° 8' and 50° 51' . . . . .	40
19	S <sub>8</sub> calculation of the thermal neutron spectra for 2.5 in. of liquid hydrogen at angles of 67° 48' and 82° 45' . . . . .	41

# LIST OF FIGURES (Contd)

<u>Figure</u>		<u>Page</u>
20	$S_8$ calculation of the thermal neutron spectra for 4.5 in. of liquid hydrogen at angles of $28^{\circ}8'$ and $50^{\circ}51'$ . . . .	42
21	$S_8$ calculation of the thermal neutron spectra for 4.5 in. of liquid hydrogen at angles of $67^{\circ}48'$ and $82^{\circ}45'$ . . . .	43
22	$S_8$ calculation of the thermal neutron spectra for 7.0 in. of liquid hydrogen at angles of $28^{\circ}8'$ and $50^{\circ}51'$ . . . .	44
23	$S_8$ calculation of the thermal neutron spectra for 7.0 in. of liquid hydrogen at angles of $67^{\circ}48'$ and $82^{\circ}45'$ . . . .	45
24	Intermediate neutron spectrum calculations for 2.5 in. of liquid hydrogen . . . . .	50
25	Intermediate neutron spectrum calculations for 4.5 in. of liquid hydrogen . . . . .	51
26	Intermediate neutron spectrum calculations for 7.0 in. of liquid hydrogen . . . . .	52
27	Intermediate neutron spectrum calculations for 10.5 in. of liquid hydrogen . . . . .	53
28	Intermediate neutron spectrum calculations for 13.0 in. of liquid hydrogen . . . . .	54
29	Flight path configuration for thermal neutron experiments.	56
30	LH <sub>2</sub> cryostat showing cadmium covering . . . . .	58
31	Uranium source and support, beam tube guide, aluminum slug monitor and holder, and mirror used for monitoring electron beam . . . . .	59
32	Photograph of uranium source . . . . .	60
33	Flight path configuration for fast neutron experiments . .	62

## 1. INTRODUCTION

This is the third quarterly report of the work being performed on the measurement of neutron spectra in liquid hydrogen for the National Aeronautics and Space Administration under Contract No. NAS 3-6217. This report covers the period from December 18, 1965 to March 17, 1966.

## 2. LIQUID HYDROGEN FACILITY

A major effort on this program was the setup, or more accurately the resetup, of the liquid hydrogen facility since the facility had been set up for previous use on Contract NAS 3-4214. This setup was necessary prior to doing any time-of-flight neutron spectral measurements in liquid hydrogen ( $\text{LH}_2$ ).

The setup of the  $\text{LH}_2$  facility was completed during this quarter. Although details of this setup were discussed in the second quarterly report (NASA CR-54889) a synopsis will be included herein. However, emphasis will be placed on those items which were completed during this quarter. These include the reinstallation of all safety devices, and operating experience gained during the first series of neutron spectrum measurements.

The liquid hydrogen facility is composed of the following components:

- a. Remote control liquid hydrogen console
- b. Liquid hydrogen cryostat and support structure
- c. Valve package
- d. Gas cylinders or tube trailer and the associated plumbing for distributing the gaseous nitrogen or gaseous helium (commonly referred to as the "bottle farm").

- e. Connections from the  $\text{LH}_2$  cryostat to the valve package such as the flexible vent lines and the vacuum jacketed fill and dump line.
- f. Vacuum jacketed transfer lines from the valve package to the  $\text{LH}_2$  supply dewar.
- g. Sheet metal enclosure and work platform.

### 2.1 Remote Control Liquid Hydrogen Console

The liquid hydrogen console, which is remotely located in the data room, is the control center for all valves. A photograph of the console is shown in Fig. 1.

The  $\text{LH}_2$  console also performs a number of other functions, many of which are associated with safety devices which are discussed below.

One panel on the console contains a schematic of the flow of gaseous or liquid hydrogen and lights indicate the position of the valves (open or closed) which control this flow.

Another panel contains the controls for remotely-operated valves for purging the sheet metal enclosure around the  $\text{LH}_2$  cryostat. In case of fire this enclosure can be purged with an inert gas to preclude the entry of oxygen. On the previous contract (NAS 3-4214) carbon dioxide supplied from a dewar was chosen for this gas. However, at the flame temperature of hydrogen, carbon dioxide can break down into carbon monoxide and oxygen. Since this was considered unsafe, approval was asked and permission was granted by the Project Manager, John Liwosz, to rent a nitrogen dewar and buy the nitrogen to fill it. A 160-gallon, 100-psi maximum pressure liquid nitrogen dewar was rented from Linde and the existing  $\text{CO}_2$  piping system to the valve package and cryostat areas was modified to fit the new dewar. This system performed satisfactorily;

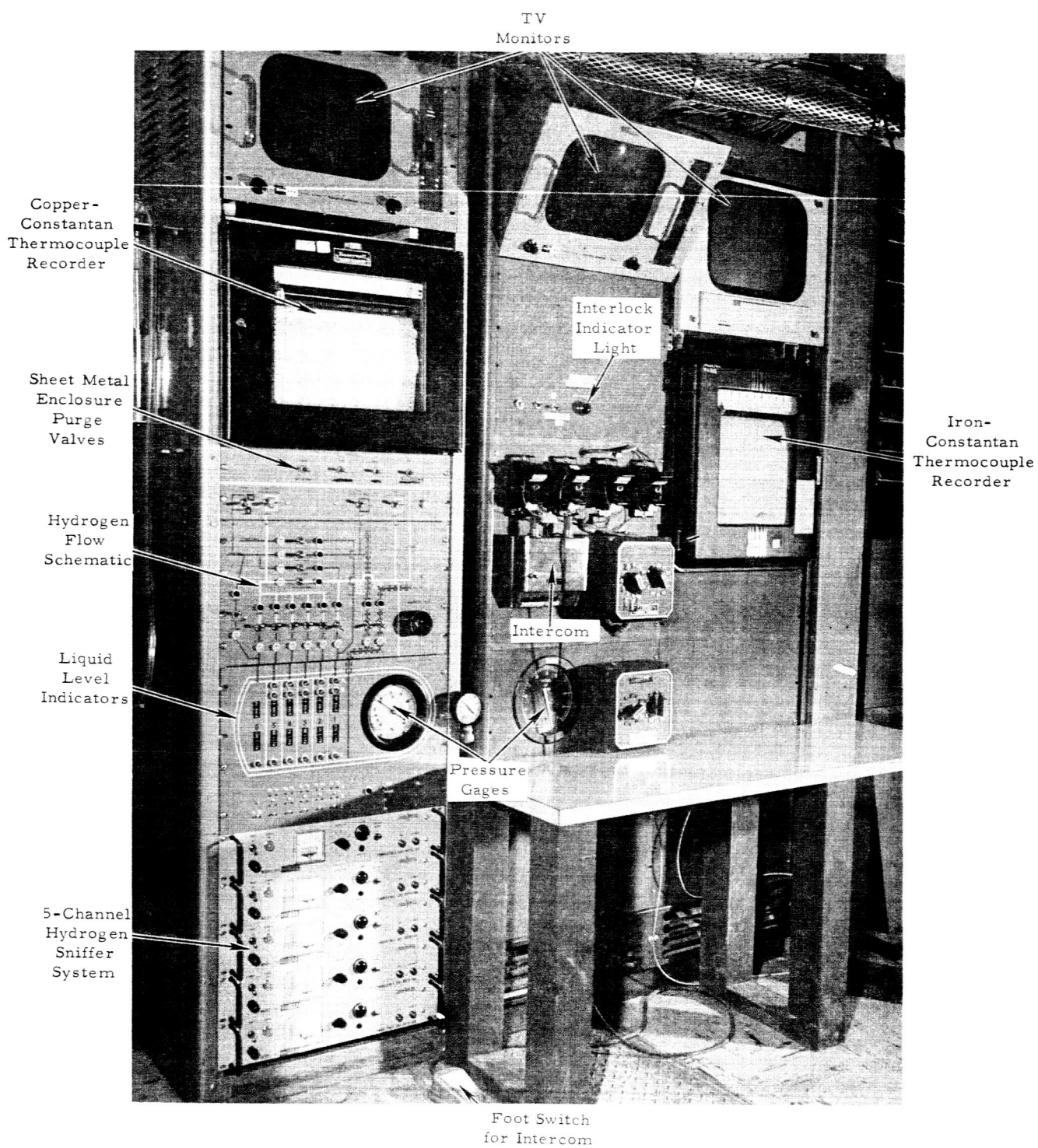


Fig. 1--Liquid hydrogen console

it required only about 35 seconds at 60 psi dewar pressure to flood the sheet metal enclosure with cold gaseous nitrogen. Carbon dioxide had also been used for a fire fighting system to control possible fires in the  $\text{LH}_2$  supply dewar area. Since this area is open the use of carbon dioxide is permissible;  $\text{CO}_2$  gas cylinders equipped with nozzles were placed in this area. A fire in the  $\text{LH}_2$  supply dewar area could also have been controlled by water hoses located about 100 ft from the supply dewar.

The  $\text{LH}_2$  console also contains 16 liquid level indicators for either  $\text{LN}_2$  or  $\text{LH}_2$ . The liquid level indicators utilize 1/4-watt, 1000-ohm, carbon composition resistors as liquid level sensors. The unbalance of a bridge circuit is used to indicate the level of the liquid. Each carbon resistor is backed by two duplicate resistors. One set of these resistors was monitored with a Wheatstone bridge and was extremely useful during filling, dumping, and transferring of the liquid from one chamber to another.

An intercom system connects all of the remote areas with the console. A voice-operated relay was originally planned to free the operator of the  $\text{LH}_2$  console from manual operation of the intercom during critical operations. However, this system was not satisfactory because of background noise and a foot switch was used instead.

Three TV monitors located at the  $\text{LH}_2$  console were used. One monitor was used to view the electron beam spot position in the hole of the uranium source and to determine positive seating of the aluminum monitor slug holder. The second monitor viewed the vent line connections and fill/dump line connection at the top of the dewar. This monitor would have determined if a break had occurred at these connections. The third TV monitor was used to verify position of the  $\text{B}^{10}$  background plug. Since the  $\text{LH}_2$  cryostat has a very small ullage space,  $\text{LH}_2$  can easily be entrained in the nonvacuum jacketed vent lines and cause liquid oxygen to form on these lines. This condition can also be caused by the flow of cold hydrogen gas through the vent lines. Therefore, the third

monitor was also used to observe the vent lines to determine if liquid oxygen was being formed on the vent lines.

The uranium source is water-cooled and is interlocked with the electron linear accelerator interlock system by means of a flow switch in the water system. In case of a water leak or rupture the Linac is automatically shut off and a light on the  $\text{LH}_2$  console indicates the interlock has been interrupted.

Two sets of thermocouples are used to monitor temperature. Copper-Constantan thermocouples were used to determine the temperature of the liquid hydrogen in three positions of Chamber One of the  $\text{LH}_2$  cryostat. This type of thermocouple was also used to determine the temperature of the six vent line connections at the dewar and the temperature of the vent lines at the lowest points of vent lines Number One and Two.

Iron-Constantan thermocouples were used to determine the presence of fire at the dewar, valve package,  $\text{LH}_2$  supply dewar, dump, and/or vent lines. The Iron-Constantan thermocouples were also used to monitor the temperature of the uranium source. The recorder for measuring the Iron-Constantan thermocouples was interlocked with the Linac so that if the temperature should exceed  $500^\circ\text{F}$  the Linac would automatically be shut off. The same visual indicator as for the water supply for the uranium source would note this condition and steps would then be taken in accordance with our "Emergency Procedures."

Following Dr. John Liwosz's (Project Manager) approval hydrogen sniffers were ordered from General Monitors, Inc. This hydrogen sniffer system consisted of five channels; three of the channels not located in a radiation field used thermistors as the sensing heads, while the two channels located in the radiation field used bifilar platinum wire sensing elements as were used on the previous contract (NAS 3-4214). The monitor for these hydrogen sniffers is located at the  $\text{LH}_2$  console shown in Fig. 1. The thermistor sensing elements were placed above and between

the  $\text{LH}_2$  cryostat and valve package inside the sheet metal enclosure and near the ceiling just outside the enclosure. The bifilar platinum wire sensing elements were placed about 4 ft up the 18-in. diameter ceiling exhaust duct for the sheet metal enclosure, at the dump and vent line exit at the top of the Linac experimental building, and at the  $\text{LH}_2$  supply dewar position. During the first series of neutron spectrum measurements, the  $\text{LH}_2$  supply dewar developed a hydrogen leak at the packing around the manually-controlled fill-drain valve and it was quickly detected by the hydrogen sniffer at that location averting a possible hazardous situation.

## 2.2 Liquid Hydrogen Cryostat and Experimental Facility

### 2.2.1 Sheet Metal Enclosure and Work Platform

On the previous contract (NAS 3-4214), the dewar and valve package area were enclosed by walls made of conducting plastic (velostat) to isolate this area from the rest of the experimental room and to provide rapid air changes in the areas where a hydrogen leak would most probably occur. It was believed that a sheet metal enclosure following the outline of the original plastic walls would provide a safer, more satisfactory structure. Therefore, 0.040-in. aluminum sheeting was used to enclose the area; however, the conducting plastic was retained in some areas to provide flexible ports for the uranium source and pure air entrances. Clear mylar sheets were used to cover ports in the aluminum walls through which TV cameras monitored conditions at the vent lines, background plug, and the  $\text{LH}_2$  cryostat top area. The enclosure is shown in Fig. 2. The concrete floor inside the enclosure was covered with aluminum sheets and all areas enclosed by the sheet metal enclosure were grounded so that the resistance was less than one-fifth of an ohm between any of the parts.



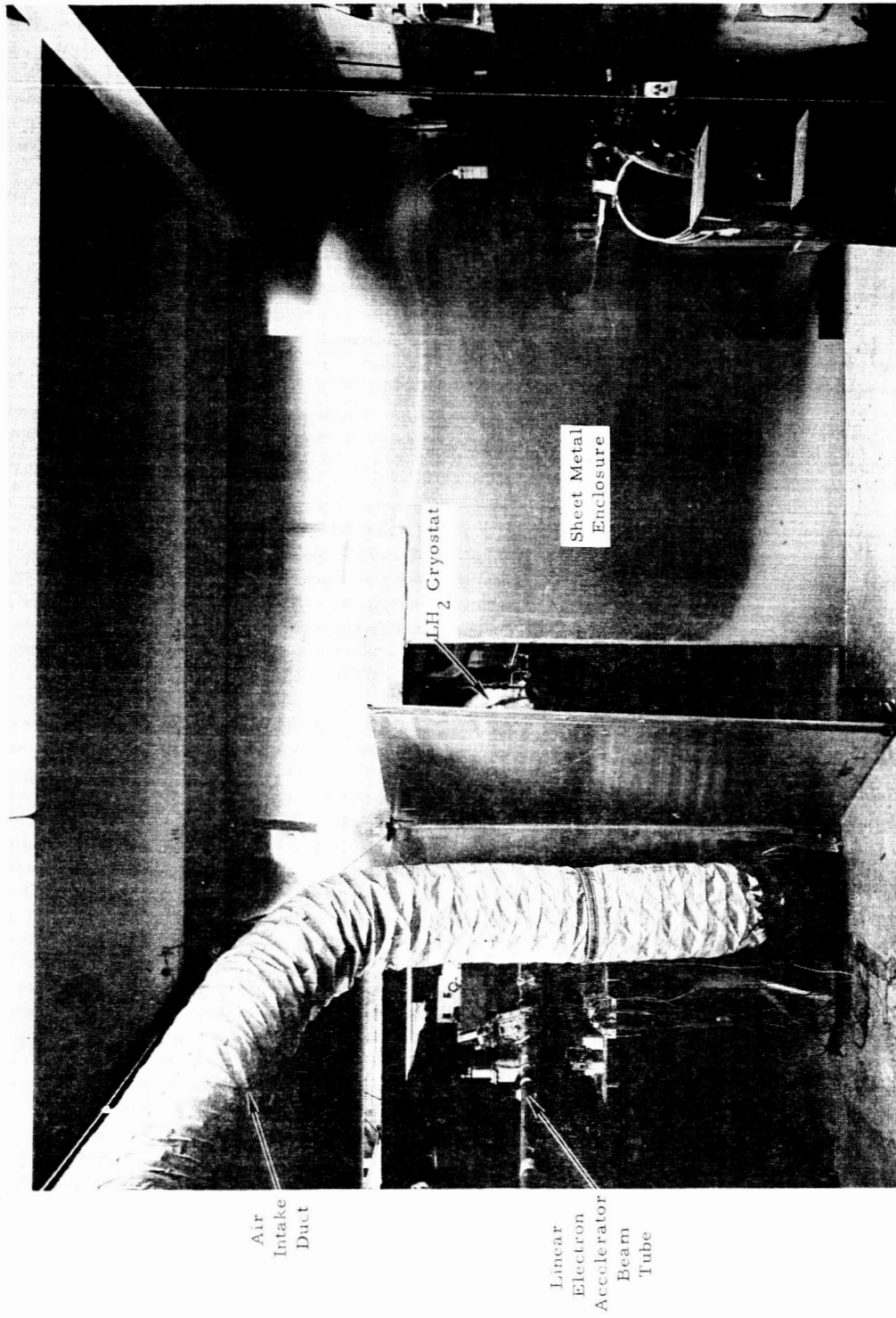


Fig. 2--Sheet metal enclosure showing flexible ducting for intake air supply

A large work platform, 6.5 ft off the floor, was erected between the dewar and the valve package to allow easy access to the valve package and the upper area of the dewar. This platform permits us to set the dewar angle without disturbing the dewar alignment, and it also provides a point of support for the vent lines.

### 2.2.2 Ventilation

An 18-in. diameter flexible duct was used as the air intake supply (see Fig. 2) for the sheet metal enclosure. Coming from this duct are two 4-in. diameter "elephant trunk" ducts which purge the areas enclosed by the roof support columns on either side of the sheet metal enclosure. The exhaust for this enclosure is an 18-in. diameter duct through the 1-ft thick concrete, 8-ft thick dirt ceiling of the experimental room. A special explosion-proof motor and static-free pulley belt were installed for use on the exhaust system for the  $\text{LH}_2$  experiments. The exhaust system is generally used for the entire experimental area, and by restricting the volume of air exchange to the sheet metal enclosure a rapid air change was achieved.

### 2.2.3 Liquid Hydrogen Cryostat Support System

A lack of rigidity in the original dewar support system caused misalignment problems during the 1964 series of  $\text{LH}_2$  experiments under the previous program. These problems occurred mainly during rotation of the dewar when a change in the center of gravity would shift the weight of the assembly on the support table and cause the probe tube pivot centerline to go out of plumb. The design of the aligning and locating devices made it difficult and time consuming to realign the dewar. Also, the single cantilever cryostat support was not rigid enough and the weight of the liquid hydrogen in the dewar would visually affect the dewar position. Therefore, a new

two-column dewar support was designed and constructed to eliminate the difficulties inherent in the older system. The new support system is shown in Fig. 3. One of the main advantages of the new system is its rigid attachment to the floor. By bolting the large diameter support columns directly to the floor, the mislocating tendencies of the previous rail-mounted table were eliminated. The two-column cantilever support system limits any weight-induced deflection to a vertical direction so that the probe pivot tube is freed of any cocking tendency. Prior to the transfer of the dewar from its old support to the new, the new system was tested by hanging a 4000-lb load on the support; only a small vertical deflection was observed for this load which was almost twice the load placed on the support system by a dewar filled with liquid hydrogen. The support system was also loaded with a 1000-lb weight, which approximates the weight of the dewar filled with liquid hydrogen. Only a 0.028-in. deflection was observed with the 1000-lb load. Thus, the 80 lb anticipated weight change between an empty dewar and one filled with  $\text{LH}_2$  caused a negligible amount of deflection in the vertical direction.

The Timken bearing originally supplied by Cryogenic Engineering Company (Cryenco) was retained at the top of the dewar, while the lower trunnion was fixed and used as a rotation locking point. This lower trunnion had been free in the Cryenco design and it was relatively easy to move the dewar out of horizontal alignment and plumb. In the new system the vertical trunnion axis is restrained and it is almost impossible to move the dewar out of plumb.

Wedge plates are used at the top of the support to provide the necessary horizontal adjustment.

During actual operation, it was observed that rotation of the dewar did not disturb the plumb of the probe tube pivot; initial alignment was relatively easy and fast and subsequent checks of the alignment showed no shifts.

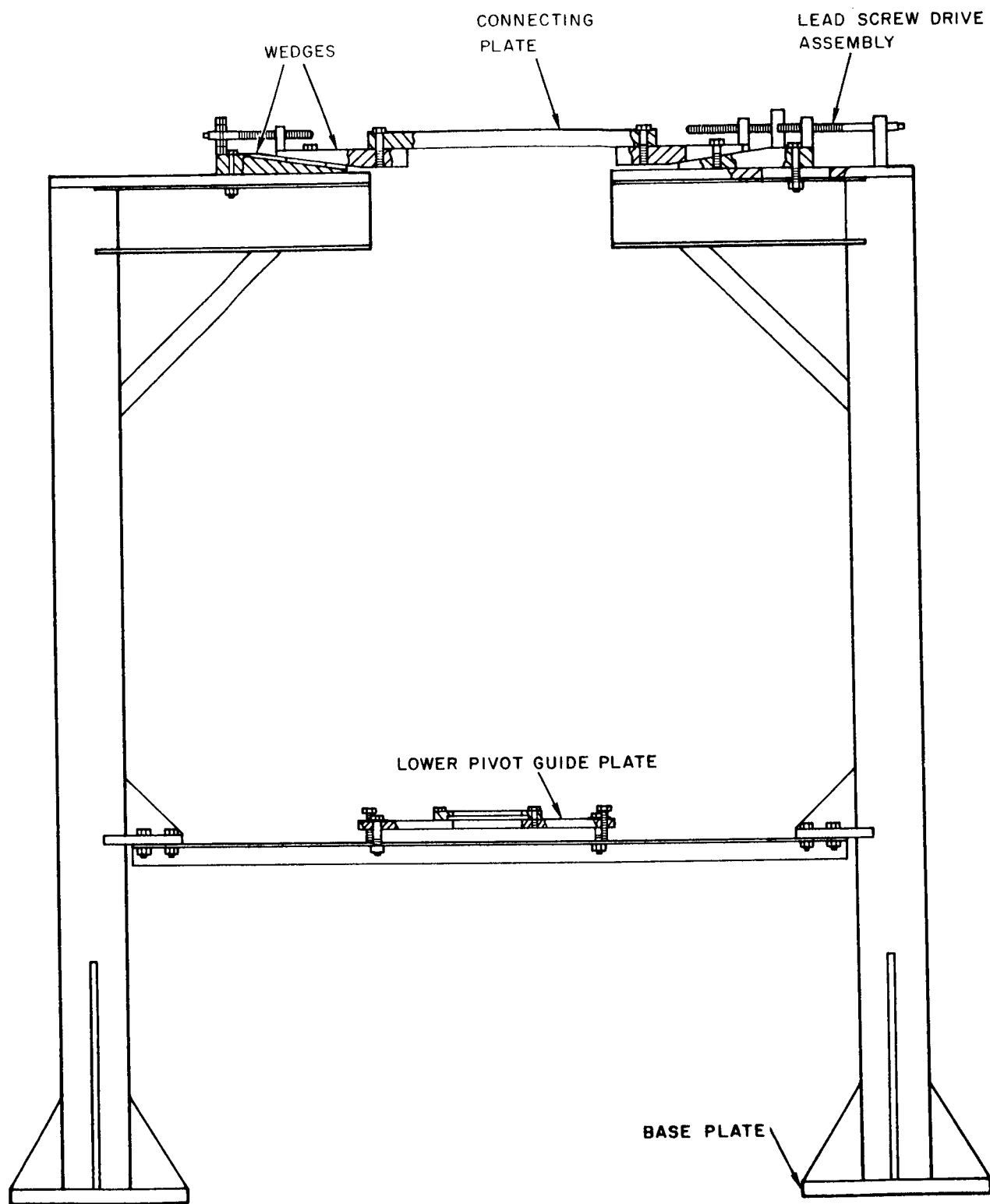


Fig. 3--Liquid hydrogen support structure. Lateral movement is provided by the lead screw drive assembly

#### 2.2.4 Vacuum

A vacuum of  $1.8 \times 10^{-5}$  mm of Hg had been obtained on the multi-layer insulation space on the  $\text{LH}_2$  cryostat as reported in the last quarterly report (NASA CR-54889) and was adequate for the experiment. Consideration had been given to trying to improve this vacuum when the cryostat was in position for the  $\text{LH}_2$  measurements since this improves the insulation properties of the cryostat. However, our program schedule did not permit improvement of the vacuum. Nevertheless, the existing vacuum proved to be more than adequate since the boiloff rate was so low that it was not detectable over a period of about ten minutes on a pressure gage that read from 0 to 50 in. of water.

#### 2.2.5 Valve Package

The cleaning of the valve package and subsequent checkout of the valve was discussed in the previous quarterly report and will not be discussed here. A close-up photograph of the valve package is shown in Fig. 4.

#### 2.2.6 "Bottle Farm"

The "bottle farm" is an array of nitrogen bottles and a helium tube trailer which are used for purging and for supplying the valve drivers. Since two types of purging are required two separate systems must be used. A third system is also used for supplying the valve drivers and a constant purge for various pieces of electrical equipment. One system acts as an emergency supply for quick dumping of the  $\text{LH}_2$ , heavy purging of the vent and dump lines, and transfer of the  $\text{LN}_2$  or  $\text{LH}_2$  within the cryostat. The other system supplies a small constant purge on the dump and vent lines and when necessary on the cryostat. Gaseous nitrogen is

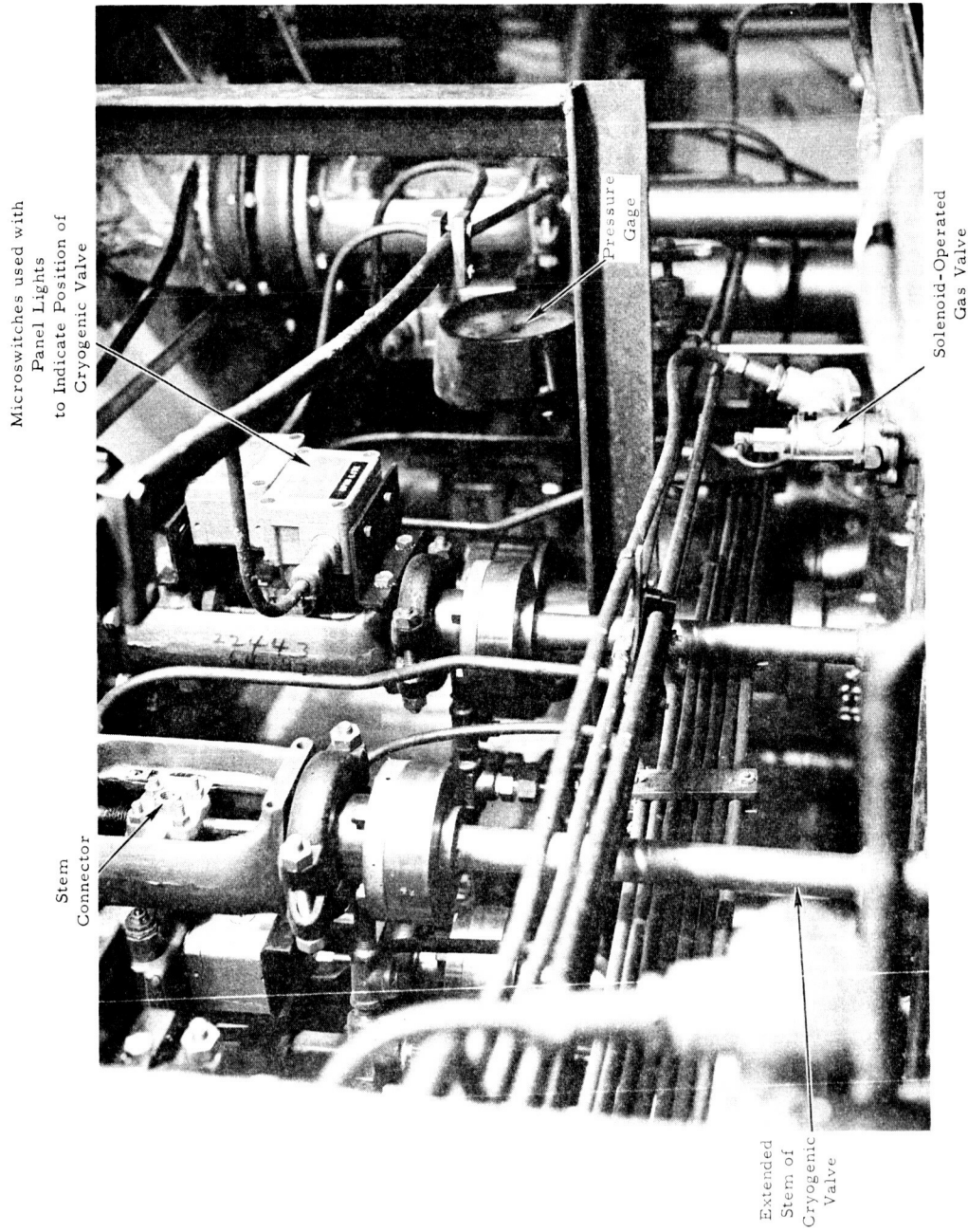


Fig. 4--Close-up photograph of valve package

used for the  $\text{LN}_2$  runs and gaseous helium for the  $\text{LH}_2$  runs. The third system, which is used for the valve drivers and purging electrical equipment, always uses gaseous nitrogen. The "bottle farm" area is shown in Fig. 5.

The gas piping system and its controls were redesigned for the present series of runs to provide a simpler, more easily read control panel to lessen operator indecision or possibility of mistakes during an emergency condition. Since the gaseous helium supply system was changed from cylinders to a tube trailer, the helium piping system was revised to accomodate the new trailer. New gaseous nitrogen lines were run to the uranium source cooling-water pump and to the three TV cameras, all of which were enclosed in conducting plastic shrouds to provide a constant nitrogen atmosphere at a slight positive pressure around these possible ignition sources. The Linac bending, steering, and focusing magnets were also purged in the same manner. A schematic of the revised piping system is shown in Fig. 6.

#### 2.2.7 Connections from $\text{LH}_2$ Cryostat to Valve Package

Five new 1/2-in. diameter vent lines were made to replace the original lines since one of the original lines was found to have several small leaks, possibly due to excessive short radius bending. The new lines were made 6 in. longer than the original lines to allow more flexing freedom. In actual operation, the new, longer lines proved to be much easier to handle and allowed greater freedom during dewar rotation.

#### 2.2.8 Vacuum Jacketed Transfer Lines from the Valve Package to the $\text{LH}_2$ Supply Dewar

The two 25-ft long transfer lines purchased from Cryenco to replace the transfer lines borrowed from Convair Division General Dynamics for the 1964  $\text{LH}_2$  experiments were received on February 7 and found to

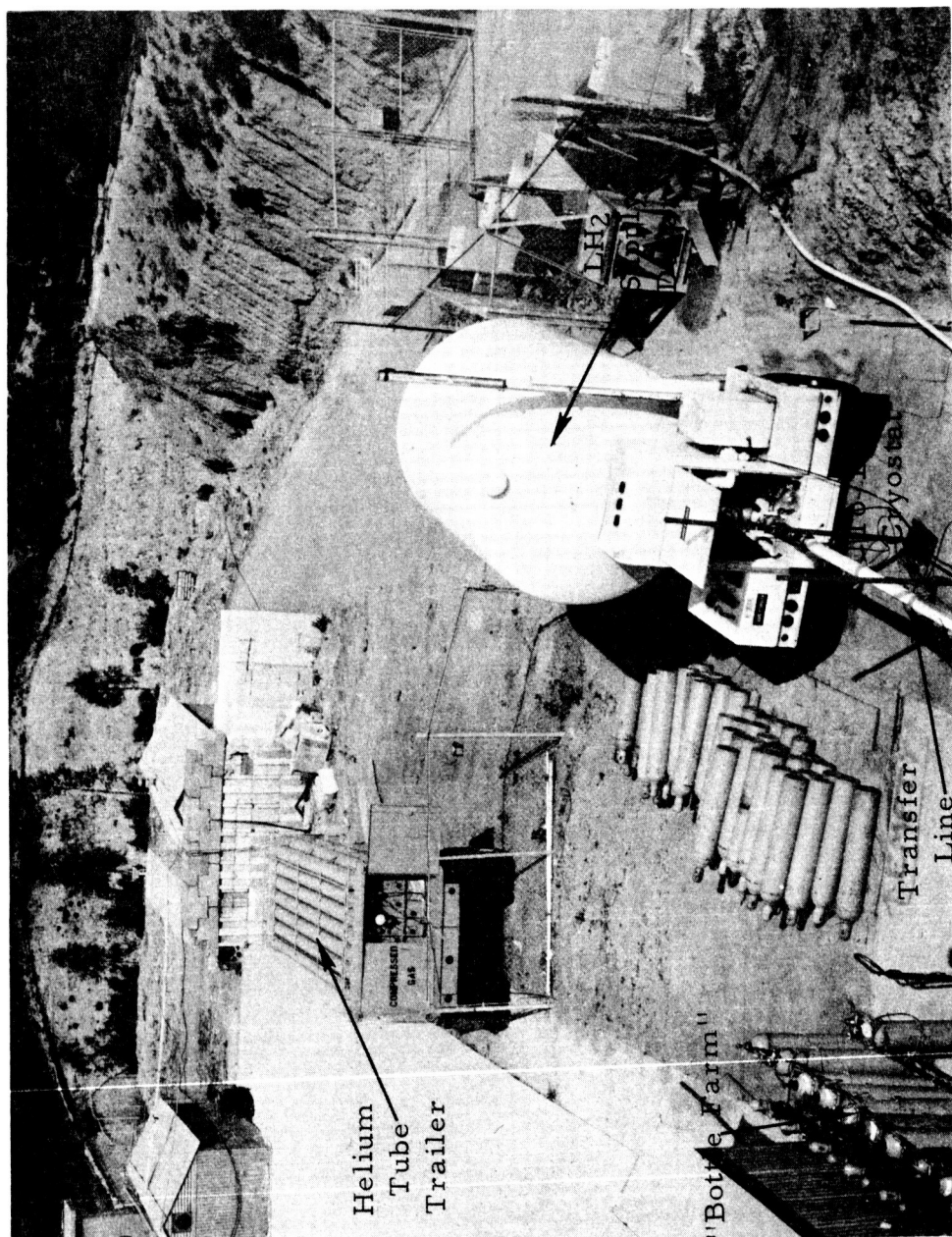


Fig. 5 -- "Bottle farm" area showing the LH<sub>2</sub> supply dewar and helium tube trailer



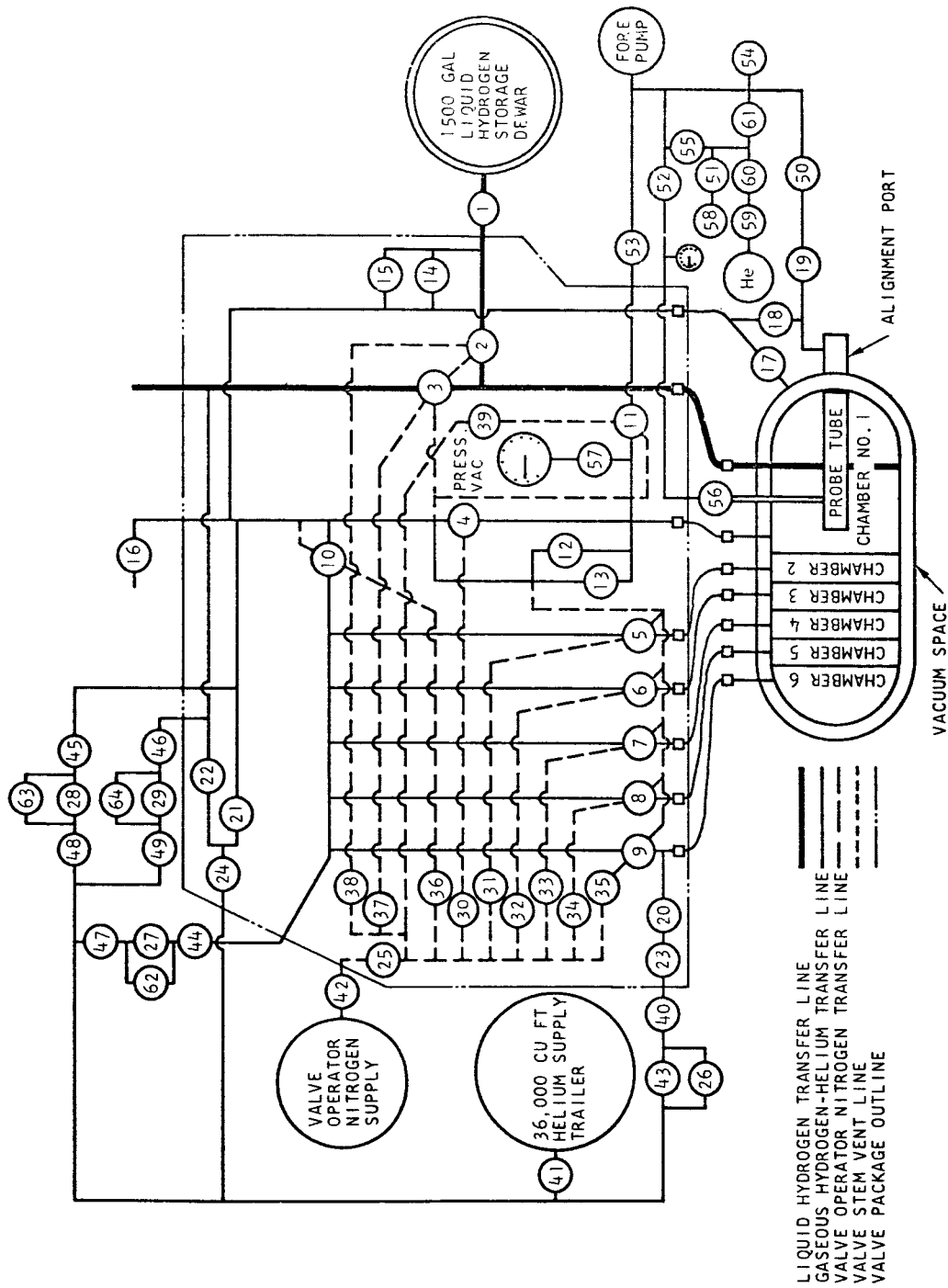


Fig. 6--Revised valve and piping system schematic

LEGEND FOR FIGURE 6

<u>Number</u>	<u>Normal Position</u>	<u>Valve</u>
1		Storage dewar hand valve
2	NC *	Dewar fill valve - BS&B vacuum jacketed 3/4" pneumatic valve
3	NO **	Dewar dump valve - BS&B vacuum jacketed 3/4" pneumatic valve
4	NC	Chamber No. 1 vent valve - BS&B extended stem 2" pneumatic valve
5	NC	Chamber No. 2 vent valve - BS&B extended stem 3/8" pneumatic valve
6	NC	Chamber No. 3 vent valve - BS&B extended stem 3/8" pneumatic valve
7	NC	Chamber No. 4 vent valve - BS&B extended stem 3/8" pneumatic valve
8	NC	Chamber No. 5 vent valve - BS&B extended stem 3/8" pneumatic valve
9	NC	Chamber No. 6 vent valve - BS&B extended stem 3/8" pneumatic valve
10	NO	Chamber No. 2 - No. 6 isolation valve - BS&B extended stem 3/4" pneumatic valve
11	NC	Vacuum purge valve - BS&B extended stem 3/4" pneumatic valve
12		Rupture disk - BS&B 2" - set at 60 psig
13		Blowoff valve - Farris 2" - set at 40 psig
14		Blowoff valve - Farris 1/2" - set at 100 psig
15		Rupture disk - BS&B 1/2" - set at 150 psig
16		Vent line flapper valve
17		Cryenco dewar vacuum space relief valve
18		Cryenco alignment port vacuum space relief valve

---

\*NC - normally closed

\*\*NO - normally open

<u>Number</u>	<u>Normal Position</u>	<u>Valve</u>
19		Alignment port evacuation hand valve
20	NO	Dewar purge valve - 1/2" Skinner solenoid valve
21	NO	Vent line purge valve - 1/2" Skinner solenoid valve
22	NO	Dump line purge valve - 1/2" Skinner solenoid valve
23		Dewar purge line regulator - Fisher 1/2" valve set at 35 psig
24		Vent-dump purge line regulator - Fisher 1/2" valve set at 35 psig
25		Valve operator line relief valve - Kunkle 1/2" valve set at 55 psig
26	NO	Transfer bypass solenoid valve
27	NC	Dewar micropurge solenoid valve
28	NC	Vent line micropurge solenoid valve
29	NC	Dump line micropurge solenoid valve
30	NC	No. 1 vent operator solenoid valve
31	NC	No. 2 vent operator solenoid valve
32	NC	No. 3 vent operator solenoid valve
33	NC	No. 4 vent operator solenoid valve
34	NC	No. 5 vent operator solenoid valve
35	NC	No. 6 vent operator solenoid valve
36	NC	No. 2 - No. 6 isolation operator solenoid valve
37	NC	Dump operator solenoid valve
38	NC	Fill operator solenoid valve
39	NC	Vacuum purge operator solenoid valve
40		Dewar purge hand valve
41		Helium purge regulator valve - set at 35 psig
42		Valve operator regulator valve - set at 50 psig
43		Liquid transfer regulator valve - set at 5-8 psig
44		Dewar micropurge hand flow rate valve

<u>Number</u>	<u>Normal Position</u>	<u>Valve</u>
45		Vent line micropurge hand flow rate valve
46		Dump line micropurge hand flow rate valve
47		Dewar micropurge flowmeter
48		Vent line micropurge flowmeter
49		Dump line micropurge flowmeter
50		Alignment port hand vacuum pump shutoff valve
51		Probe tube relief valve shutoff hand valve
52		Probe tube vacuum hand valve
53		Dewar vacuum hand valve
54		Thermocouple vacuum gage readout
55		Helium probe tube hand valve
56		Probe tube hand shutoff valve
57		Vacuum-pressure gauge hand shutoff valve
58		Probe tube pressure relief valve - popoff at 20 psig
59		Helium pressure regulator valve - set at 5 psig
60		Helium shutoff hand valve
61		Helium vacuum line hand valve
62		Dewar micropurge hand bypass valve
63		Vent line micropurge hand bypass valve
64		Dump line micropurge hand bypass valve

be as ordered. These lines were scheduled for delivery on January 28, 1966, but were delayed due to the late delivery to Cryenco of a forged part required for the Camco (NBS) bayonet connector which mates to the existing transfer line. During use of these transfer lines on the first series of the 1966 runs (February 20 through 26) they performed perfectly. However, one difficulty was experienced during the hookup of the Convair Division-supplied  $\text{LH}_2$  trailer; the adaptor originally slated for use as a coupling between the new transfer lines and the trailer was misplaced and it was necessary to use two adaptors to make the coupling. Threads on one of the adaptors was in a damaged condition and had to be repaired before the junction could be made. Additional rework of the adaptors was necessary before the next  $\text{LH}_2$  runs were begun on March 16, 1966.

### 2.3 Checkout of the Liquid Hydrogen Facility Using Liquid Nitrogen

The second checkout of the liquid hydrogen facility using liquid nitrogen took place as scheduled on January 17, 1966. Several minor problems were encountered and solved, and further familiarization was gained in the operation of the facility. The new 1/2-in. diameter vent lines were installed for use during this checkout and proved to be satisfactory.

The third checkout of the facility using liquid nitrogen was performed as scheduled on February 14, 1966. Since it was conducted less than a week prior to the first series of liquid hydrogen experiments, this checkout was used as a "dress rehearsal" for the liquid hydrogen runs and as such to determine the final readiness of the facility.

### 3. WATER-COOLED ISOTROPIC FAST NEUTRON SOURCE

Expectations of low detector counting rates for some experimental configurations made it necessary to increase the heat removal capabilities of the isotropic uranium source. This permitted the electron linear accelerator (Linac) to be operated at a higher power level thereby increasing

the neutron output of the source. A new uranium source was designed using the same copper-nickel clad 3.0-in. diameter depleted uranium sphere which had produced an isotropic fast neutron source under the previous contract NAS 3-4214. A 0.030-in. thick stainless steel spherical water jacket directs cooling water over the entire outer surface of the uranium sphere in a stream 0.090-in. thick; the jacketing also directs a high flow-rate stream of water over the surface which the electron beam strikes, thus applying the maximum cooling effect to the major point of heat input. Design calculations indicated that with a water flow of six gallons per minute at a pressure of 30 psi, 1.7 kilowatts of Linac power could be removed from the source without the temperature of the uranium exceeding 250°F. Experimentally, the source has more than lived up to power removal expectations. Details of the water-cooled source are shown in Fig. 7.

One additional advantage of the water-cooling concept is the complete containment of any fission products or uranium particles, resulting from source failure, within the sealed Linac target water-cooling system. Except in the event of a water rupture a source failure would not necessitate a complete suspension of experimental operations to allow decontamination of the area since all contaminants would be kept in the water system. The source could then be replaced with an identical backup source and the experiment continued.

On January 29, 1966, a time-of-flight fast neutron spectrum was measured on the water-cooled uranium source. The neutron spectrum was measured at an angle of 94° with respect to the electron beam and is shown in Fig. 8. This neutron spectrum agrees with the fast neutron spectrum taken on May 23, 1964, for the air-cooled uranium source. The importance of this result is that the fast neutron source for the measurements on this program, in the energy range from 0.5 to 15 MeV, is the same as for the measurements performed under the previous contract.

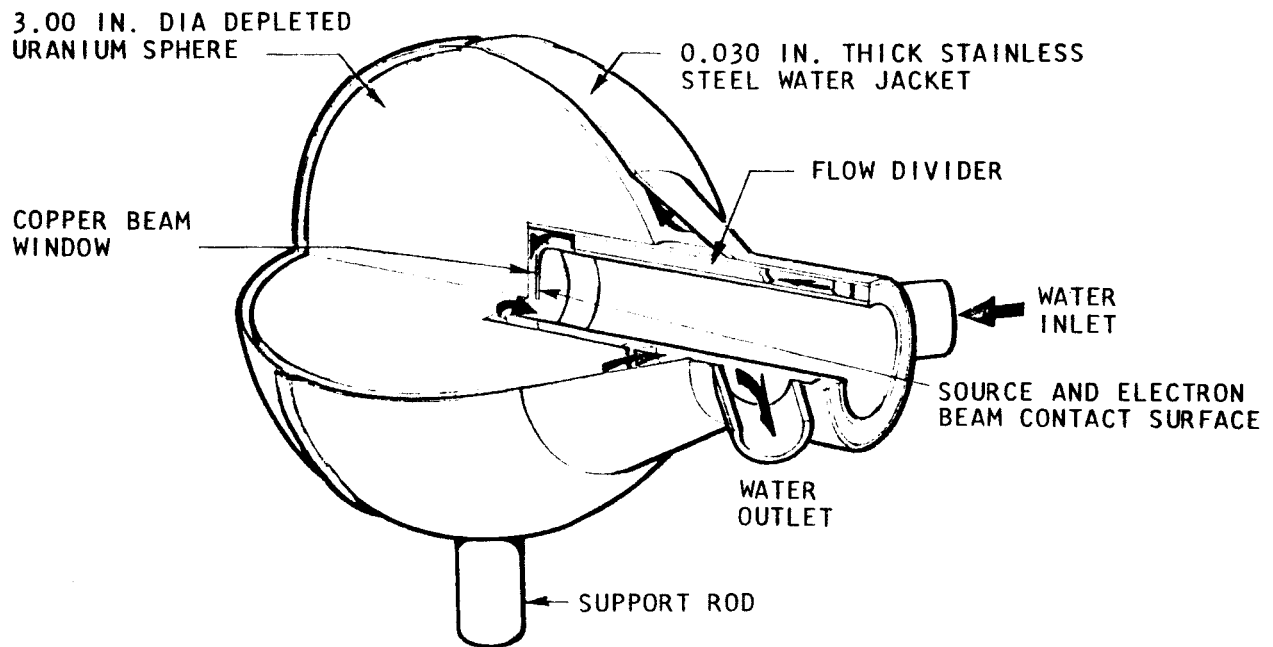


Fig. 7--Details of the water-cooled 3-in. diameter spherical uranium fast neutron source

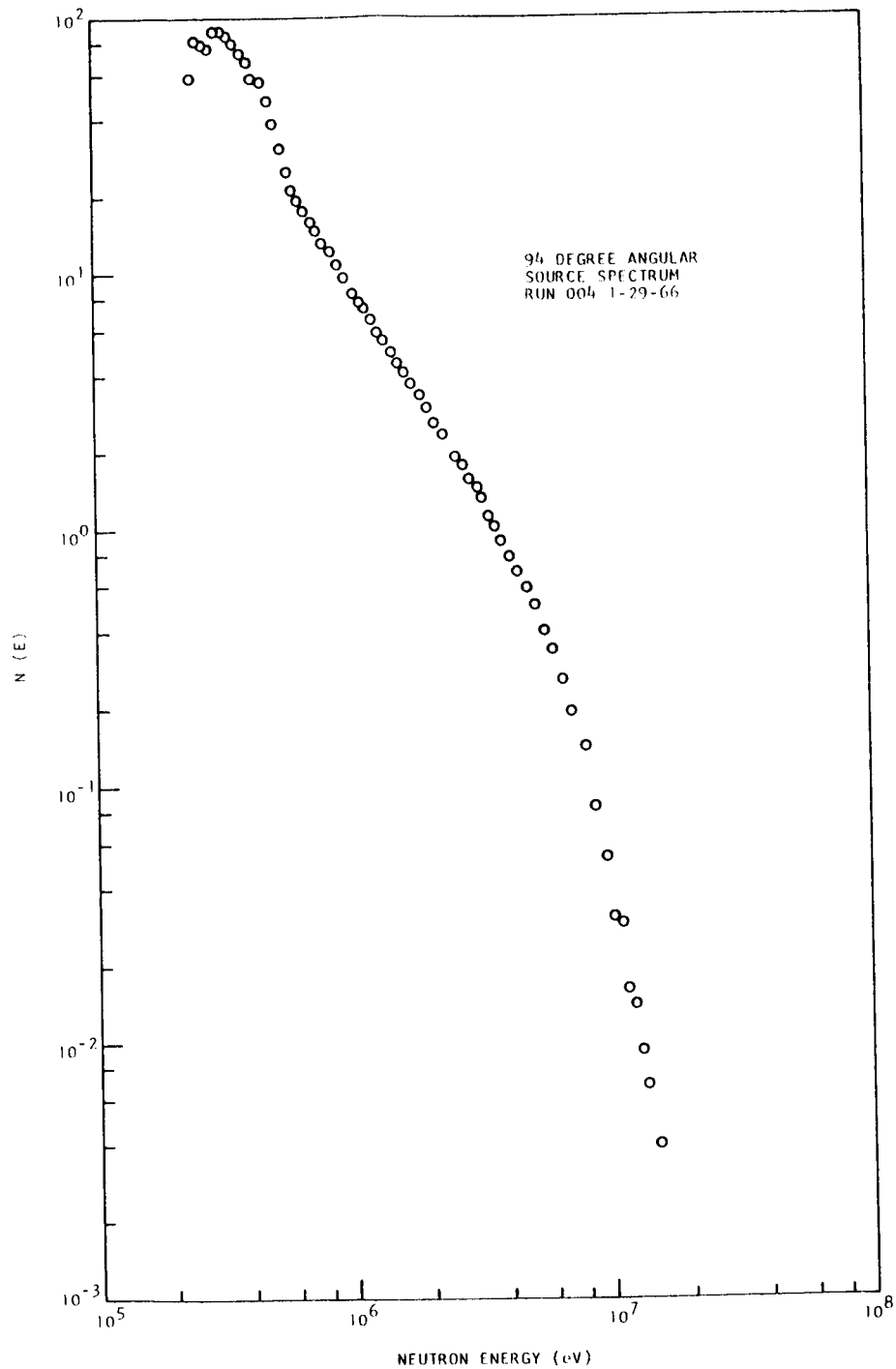


Fig. 8 - Fast neutron spectrum of a 3-in. diameter water-cooled depleted uranium source at an angle of 94°



#### 4. FAST NEUTRON SOURCE MONITORS

The main requirement of an experimental monitor is accuracy (the ability to follow from run to run the changes of source strength and to indicate these changes in direct proportion to the actual source strength variation ), It must correctly indicate flux variations over a wide range and must be insensitive to changes made in the experimental area, seeing only actual primary flux intensity changes. The monitor must be reliable, reasonably inexpensive, and fairly simple to set up or locate. Its results should be comparable on a day-to-day basis; therefore the setup, biasing, or locating procedures must be easily standardized and repeated. For the 1964 series of  $\text{LH}_2$  experiments, two types of monitors were used, an aluminum activation monitor and a U-235 fission counter. These monitors were retained for the present  $\text{LH}_2$  experiments since they had shown excellent performance characteristics during the earlier experiments.

The activation source monitors used with the present  $\text{LH}_2$  experiments were 1100 series aluminum slugs 5/8-in. diameter by 1-3/4 in. long, positioned in a new epoxy-nylon housing as shown in Fig. 9 (and as oriented with respect to the uranium source as shown in Fig. 31. Aluminum has a 7 MeV threshold for the  $\text{Al}^{27}(\text{n}, \alpha)\text{Na}^{24}$  reaction.

Because of the high activation threshold an aluminum activation monitor is relatively insensitive to albedo from the dewar material, liquid hydrogen surface, and environmental surroundings. The epoxy-nylon housing also provided some albedo shielding and guaranteed positive identical location of the aluminum slug for each run. The entire housing and monitor slug holder assembly were redesigned for the present series of  $\text{LH}_2$  experiments for easier and more positive operation. The safety requirement of no entrances to the experimental area during the presence of  $\text{LH}_2$  in the dewar forced the adoption of a remote positioning and seating device for the source monitor; the 1964 system was redesigned for more reliable operation since some difficulty had been experienced in getting

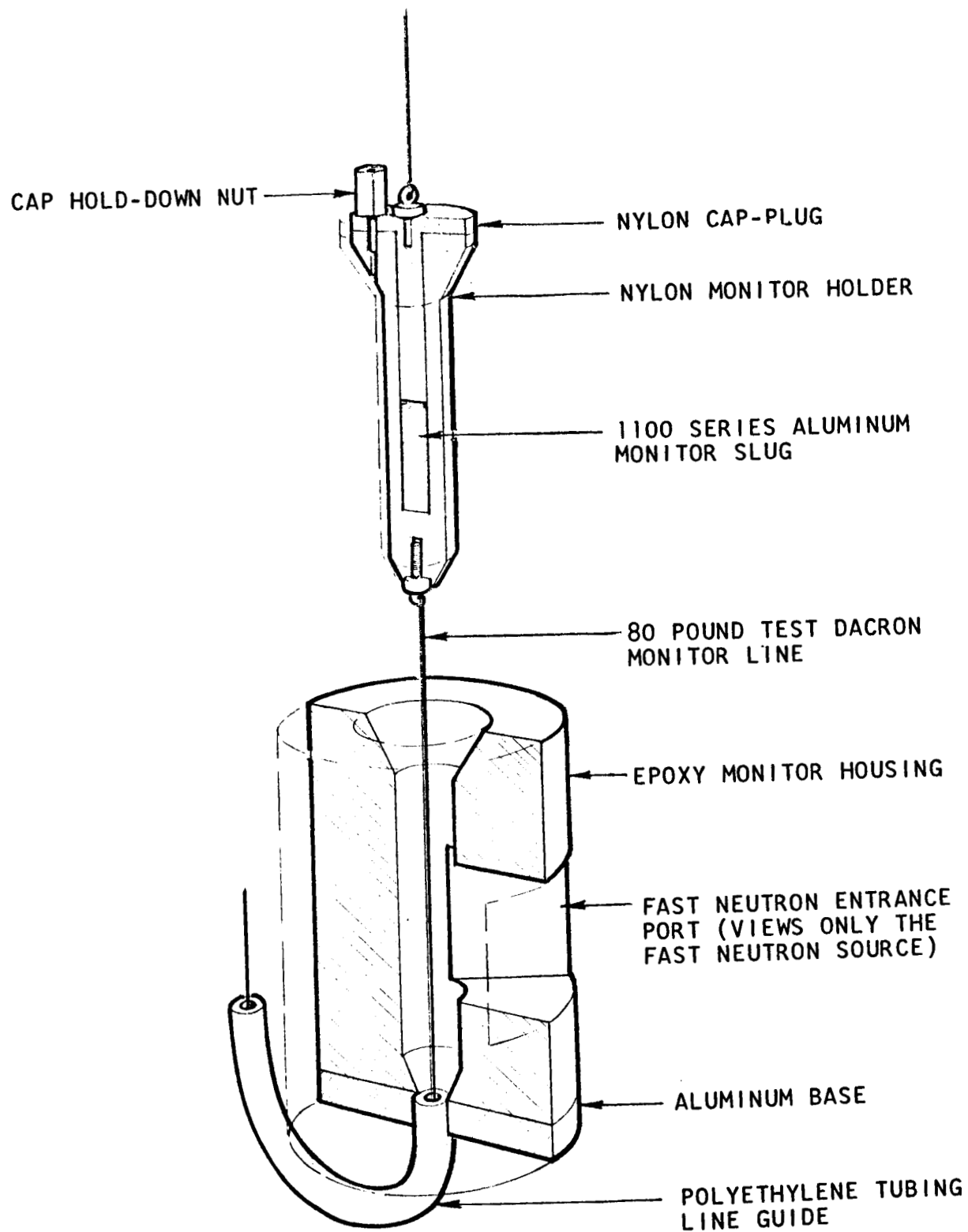


Fig. 9--Aluminum monitor system

the source monitor slug holder through the small roof passage. Handling difficulties during the changing of the slug also dictated a redesign of the slug holder. A pipe was placed in the passage to allow the monitor holder a free run without interference from the liquid level cables, thermocouple wires, and other control cables running through the roof passage. The return run of the monitor slug holder cable was through a polyethylene tubing line guide which entered the bottom of the monitor holder. A different aluminum monitor slug was used for each run.

The  $\text{Na}^{24}$  activity from the  $\text{Al}(n, \alpha)$  reaction was counted by using a well-type NaI (Tl) scintillator and conventional electronics. Great care was taken to maintain the same bias for each day. This was accomplished by taking pulse height distributions for the signal in coincidence with the discriminator output and adjusting the discriminator bias to 1 MeV. Each aluminum monitor was counted several times with at least 1% statistical accuracy to insure that the bias was adjusted for only the  $\text{Na}^{24}$  15-hour half-life activity. Some discrepancy in the dieaway of the radiation from the activated aluminum monitors was observed when the slugs were counted soon after activation. This activity had a 2-1/2-hour half-life and was probably due to  $\text{Mn}^{56}$  which occurs in trace quantities in aluminum. Since the half-life of the extraneous activity was 2-1/2 hours, the aluminum monitors were reliably counted sixteen or more hours after irradiation.

The alternate monitor used on the  $\text{LH}_2$  experiments consisted of a small U-235 fission chamber and associated amplification electronics. This monitor was used only as an instantaneous trouble-indicating monitor and as a backup for the activation monitor.

## 5. PROBE TUBE ALIGNMENT MECHANISM

Accurate positive alignment of the experimental dewar probe tube with the flight path was essential to the acquisition of good experimental data. Due to the nature of the experiment, it was necessary to have an

alignment and support system which allowed us to initially align with a transit the dewar with the flight path. For this purpose an alignment port has been provided. However, during operation this port must be closed and the dewar rotated to any desired angle without affecting the probe tube alignment. As the new dewar support system, described in Section 2.2.3, proved to be extremely rigid and stable, it was felt that the external shaft of the probe tube could be rigidly attached to the alignment roof plate after alignment, to insure no relative motion with respect to the flight path. A somewhat modified version of the alignment system used on the previous program (Fig. 10) was designed and built. In the new system the two alignment arms are at  $90^{\circ}$  with respect to each other, while the large diameter tubes extending downward from the roof plate are a loose slip fit in the alignment arm holes (see Fig. 11). Observation of the cross hairs on the probe tube with a transit while a moderate load was applied to the dewar and to the alignment arms showed no discernable movement, indicating that alignment would be maintained even if the alignment arms were bumped. The alignment plate at the top of the dewar was machined by Cryenco so that its flat upper surface would be exactly perpendicular to the centerline of the probe pivot tube. A close tolerance bore in the center of the plate fits very tightly over a bearing surface concentrically machined at the top of the probe pivot tube. The alignment plate bearing surface is external to the dewar. During manufacture the probe tube was carefully welded to the invar pivot tube. The centerline of the probe tube is perpendicular to the pivot tube's centerline within 0.005 in. over the entire length of the probe tube. Therefore, this provided a positive method of knowing the attitude of the probe tube centerline in relation to the horizontal. During the alignment procedure, the dewar attitude was adjusted by using the leveling mechanism on the dewar support so that a precision level placed on the flat surface of the dewar alignment plate indicated dead horizontal at two positions  $90^{\circ}$  apart. The inner cross hairs on the probe

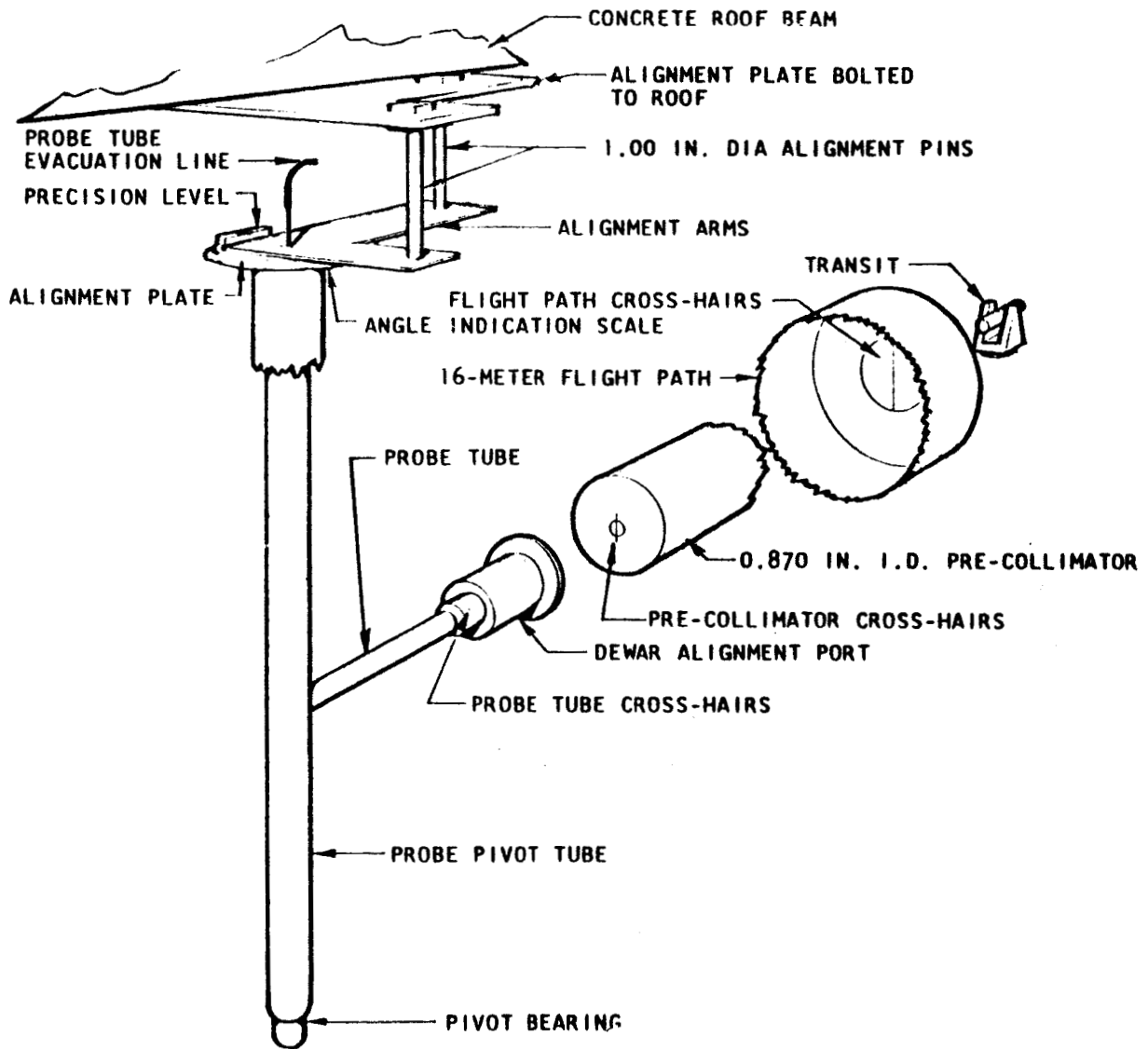


Fig. 10--Cutaway view of the probe tube alignment system

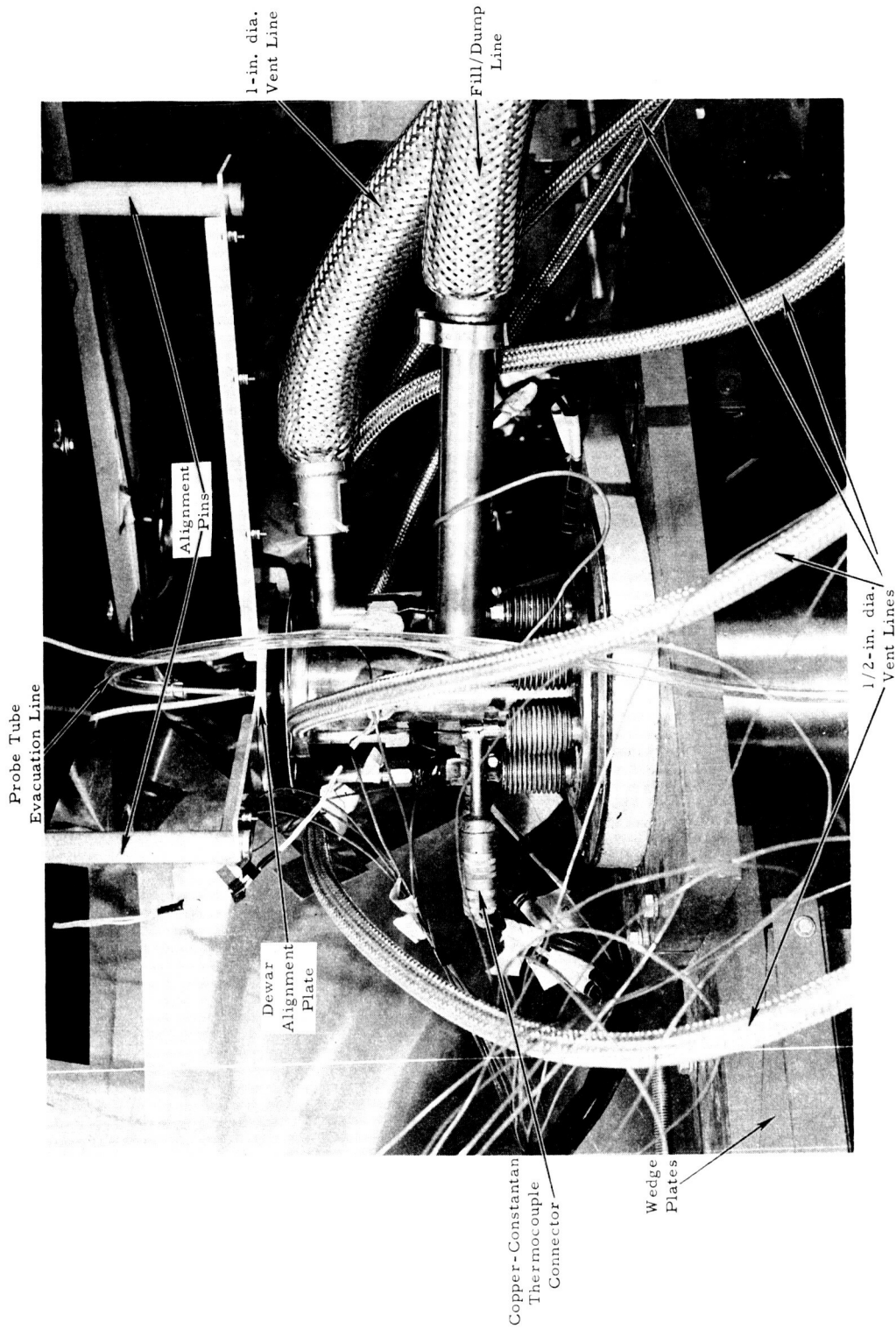


Fig. 11--Photograph of the alignment plate

pivot tube were then aligned with the flight path while the probe tube was pivoted to a position  $90^\circ$  from the flight path centerline; the probe tube was then pivoted back to the flight path centerline, the alignment tubes lined up in the alignment arms and roof plate holes, and the whole alignment assembly was then securely tightened.

#### 6. BACKGROUND PLUG USED FOR THE THERMAL NEUTRON SPECTRUM MEASUREMENTS

A means of eliminating the thermal neutron signal from the experimental dewar was needed to provide a method of determining the amount of "background" counts observed in the  $\text{BF}_3$  detector bank for each signal run. These "background" counts may be due to cosmic events and neutron transmission through the flight path shielding and collimators, and must be subtracted from the signal run to yield the true neutron spectrum originating in the  $\text{LH}_2$  dewar. The boron isotope  $\text{B}^{10}$  was used because of its high thermal neutron cross section; since the  $\text{B}^{10}$  was in powder form an aluminum container shown in Fig. 12, was built to provide a  $\text{B}^{10}$  cylinder 0.625-in. thick and 1.375 in. in diameter. The 0.625 in. thickness is sufficient to eliminate all neutrons below 300 eV.

Since our safety procedures precluded entry into the experimental area during the  $\text{LH}_2$  experiment while hydrogen was in the dewar, a remote control mechanism, also shown in Fig. 12, was constructed to introduce and remove the background plug into the flight path. The position of the plug during the experiments was verified with one of the television monitors mounted at the liquid hydrogen console.

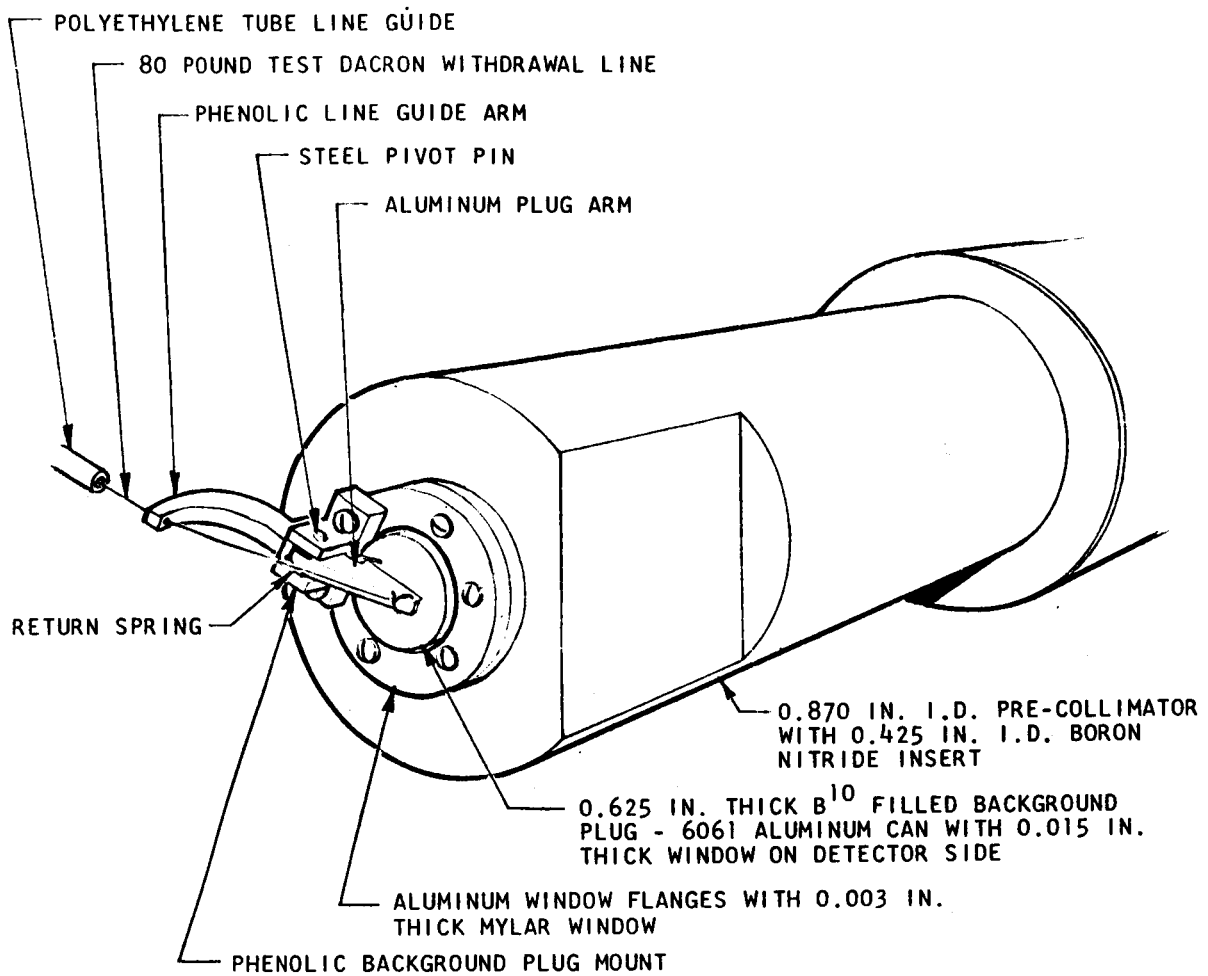


Fig. 12 --  $B^{10}$  background plug



## 7. THEORETICAL CALCULATIONS OF NEUTRON SPECTRA

### 7.1 Thermal Neutron Energy Spectrum Calculations

#### 7.1.1 Energy Levels

Energy levels were submitted to, and approved by, the Project Manager for calculations in the thermal region (0.0004 to 1 eV). These energy levels are presented in Table 1. On the basis of this approval, calculations were then made in the thermal neutron energy region, details of which are presented in the next section.

#### 7.1.2 Details of the Calculations

The  $P_0$  and  $P_1$  scattering kernels for para- and ortho-hydrogen were calculated using the code LHK<sup>(1)</sup> written for the IBM 7044 computer. LHK generates cross sections for 80 energy points, from 0.0002 to 1.0 eV. Although GAPLSN<sup>(2)</sup> calculations may be performed with this fine-group cross section, the limitations in computer storage required a fewer number of groups; a 32 broad energy group was therefore used. This group collapsing was done by averaging over a calculated flux using the GATHER-II<sup>(3)</sup> code. The stainless steel of the baffles was homogenized with liquid hydrogen. The stainless steel macroscopic cross section was generated as a  $1/v$  absorber with a value of  $0.308 \text{ cm}^{-1}$  at 0.0253 eV and a constant macroscopic scattering cross section of  $1.016 \text{ cm}^{-1}$ . The reduced atom density for liquid para-hydrogen was 0.04131 atoms/barn-cm, and for liquid ortho-hydrogen it was  $8.7 \times 10^{-4}$  atoms/barn-cm since at the boiling point of liquid hydrogen,  $20.4^\circ\text{K}$ , the equilibrium para and ortho concentrations are 99.79 and 0.21 percent respectively.<sup>(4)</sup> Since stainless steel was introduced into GATHER-II as a macroscopic cross section given above, only the volume fraction of  $1.909 \times 10^{-2}$  was used as an input.

Table 1

ENERGY LEVELS FOR  
THERMAL NEUTRON SPECTRUM CALCULATIONS

<u>Group</u>	<u>Energy Level (eV)</u>
1	1.000
2	0.850
3	0.700
4	0.550
5	0.450
6	0.360
7	0.260
8	0.180
9	0.140
10	0.1070
11	0.0830
12	0.0640
13	0.0490
14	0.0380
15	0.0292
16	0.0223
17	0.0196
18	0.0172
19	0.0152
20	0.0133
21	0.0177
22	0.0103
23	0.0090
24	0.0079
25	0.0061
26	0.0047
27	0.0032
28	0.0025
29	0.0019
30	0.0013
31	0.0008
32	0.0004

The code DSZ<sup>(5)</sup> was used to calculate the  $P_0$  and  $P_1$  components of the volume-distributed first collision thermal neutron source assuming that the spatial dependence of the epithermal flux (above some cut-off energy,  $E_c$ , in this case 1 eV) is known. The spatial dependence of the epithermal flux was assumed to be of the form

$$\varphi = \varphi_0 e^{-0.122x} \quad (1)$$

DSZ uses the total buckling,  $B_T^2$ , where

$$B_T^2 = B_{\text{Transverse}}^2 + B_{\text{Axial}}^2$$

where  $B_{\text{Axial}}^2$  is derived from Eq. (1), and

$$\begin{aligned} B_{\text{Transverse}}^2 &= \left( \frac{2.405}{R+d} \right)^2 \\ &= \left( \frac{2.405}{53.34+d} \right)^2 \\ &= 0.0019 \text{ cm}^{-2} \end{aligned}$$

where  $d$  is taken as the extrapolation distance for the highest energy group. This gives

$$B_{\text{Axial}}^2 = -0.013 \text{ cm}^{-2}.$$

The  $\text{LH}_2$  cryostat in the transverse direction is circular, the buckling being calculated on that basis although slab geometry was used for the calculations.

Since GAPLSN<sup>(2)</sup> is a one-dimensional transport theory code, the transverse buckling was added as a virtual absorber,  $D(E)B_{\text{Transverse}}^2$  where

$$D(E) = \frac{1}{3 \Sigma_{\text{tr}}(E)}$$

and  $\Sigma_{tr}(E)$  is the macroscopic transport cross section. Because of the limitation imposed by memory capacity of the computer, the virtual absorber was added to the hydrogen cross sections prior to input to GAPLSN.

Two sets of calculations were done using the one-dimensional transport theory code GAPLSN and slab geometry. The first calculation used an  $S_4$ , i. e., 4 equal angular intervals from  $\mu = -1$  to  $\mu = +1$ ;  $P_1$ ; 75 space points with a 0.5 cm spatial mesh for a total thickness of 37.5 cm (a thickness greater than 13 in. must be used since a backscattering thickness of several inches is required to make the largest thickness correct); and a 32 energy group. The mean angles for this calculation were  $39^\circ 14'$  and  $75^\circ 31'$ . This calculation used the memory capacity of the IBM 7044. The results of these calculations are presented in Figs. 13, 14, 15, 16, and 17 for the two angles  $39^\circ 41'$  and  $75^\circ 31'$  for thicknesses of 2.5, 4.5, 7.0, 10.5 and 13.0 in. The second set of calculations was made to determine the change of the thermal neutron spectra as a function of angle since the  $S_4$  calculation was limited to two mean angles between  $0$  and  $90^\circ$ . These calculations were for an  $S_8$ ,  $P_1$ , 50 space points with a 0.5 cm spatial mesh, and a 32 energy group. The memory capacity of the IBM 7044 limited this calculation to a total thickness of 25 cm which was sufficient to allow a backscattering thickness so that the 7.0-in. data would be correct. The mean angles for this calculation were  $28^\circ 8'$ ,  $50^\circ 51'$ ,  $67^\circ 48'$ , and  $82^\circ 45'$ . The results of these calculations are presented in Figs. 18, 19, 20, 21, 22, and 23. As can be seen from these figures, the intensity and spectral shape do not vary much as a function of angle and thickness.

## 7.2 Intermediate Neutron Energy Spectrum Calculations

### 7.2.1 Energy Levels

Energy levels were submitted to, and approved by, the Project Manager for calculations in the intermediate neutron energy region

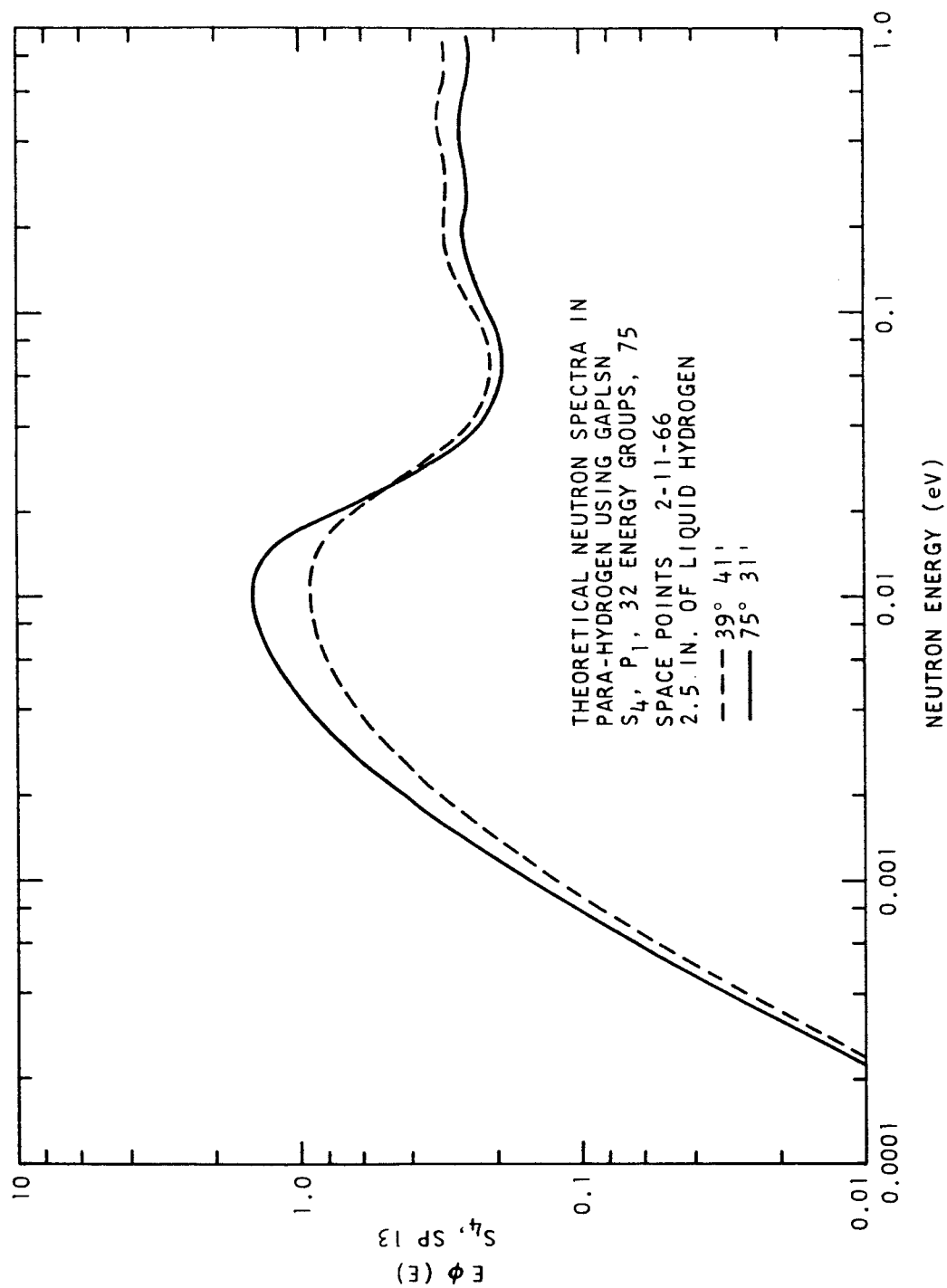


Fig. 13-- $S_4$  calculation of the thermal neutron spectra for  
 2.5 in. of liquid hydrogen

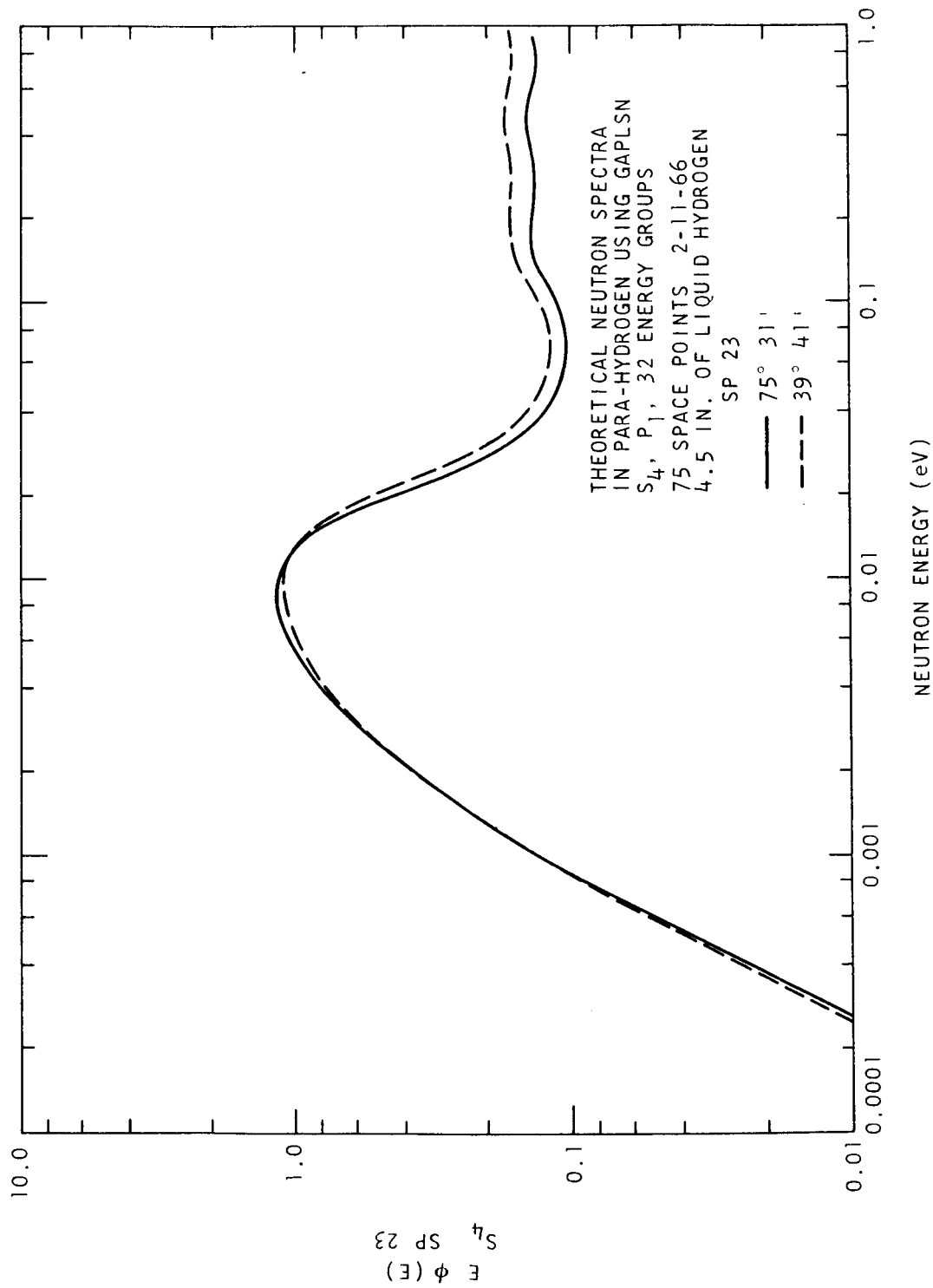


Fig. 14--S<sub>4</sub> calculation of the thermal neutron spectra for  
4.5 in. of liquid hydrogen

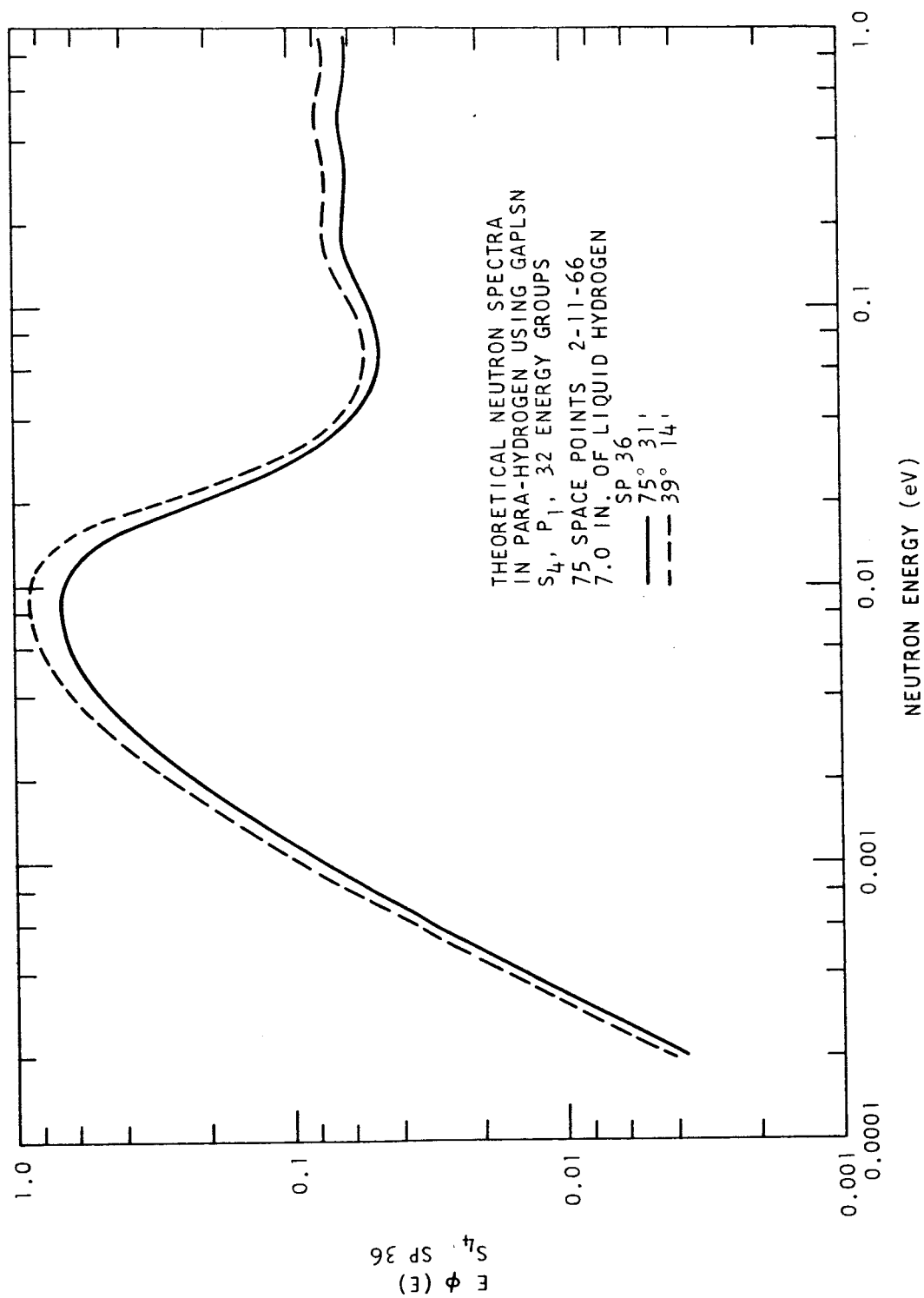


Fig. 15--S<sub>4</sub> calculation of the thermal neutron spectra for  
7.0 in. of liquid hydrogen

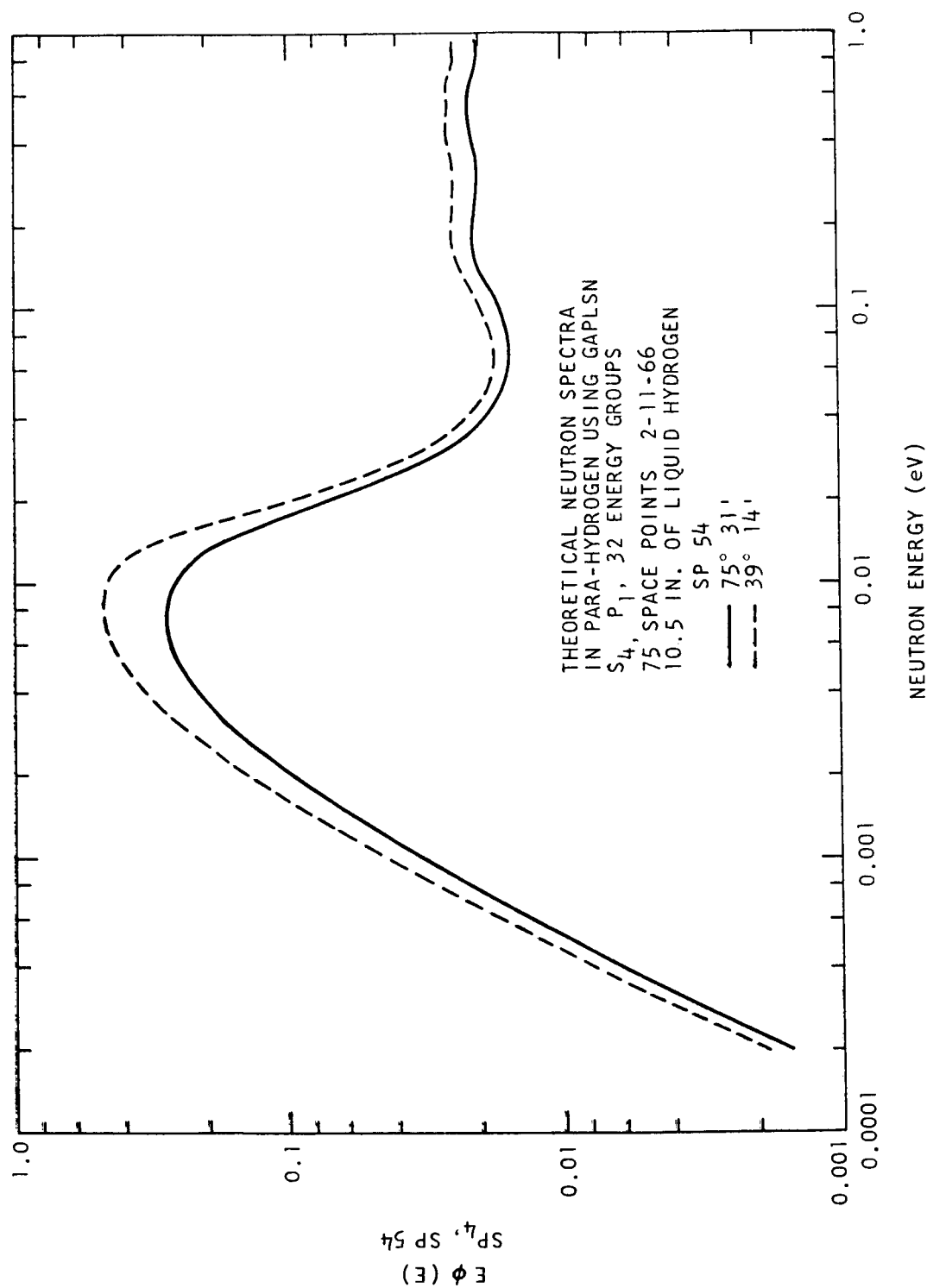


Fig. 16 -- S<sub>4</sub> calculation of the thermal neutron spectra for  
10.5 in. of liquid hydrogen



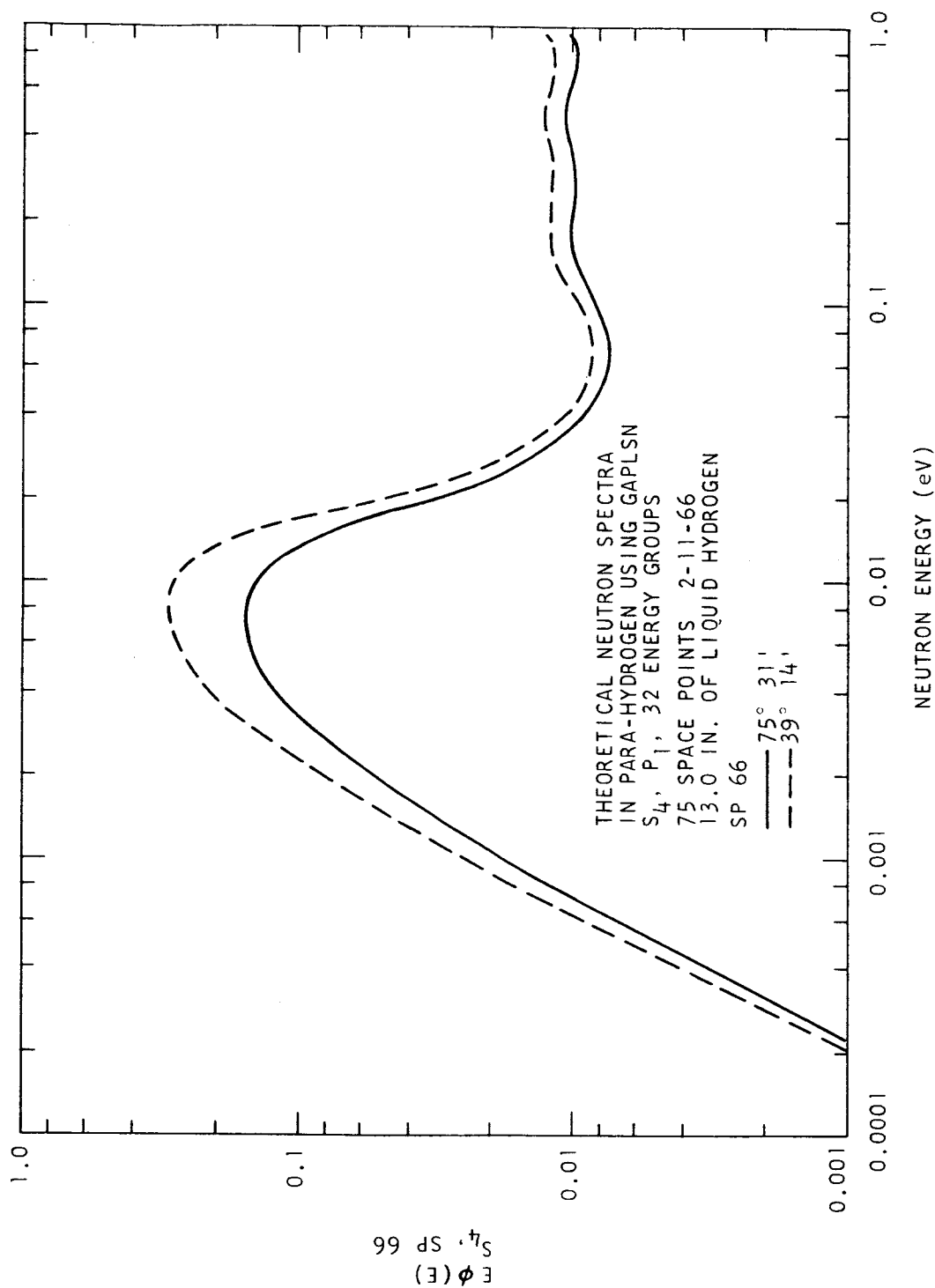


Fig. 17.--S<sub>4</sub> calculation of the thermal neutron spectra for  
13.0 in. of liquid hydrogen

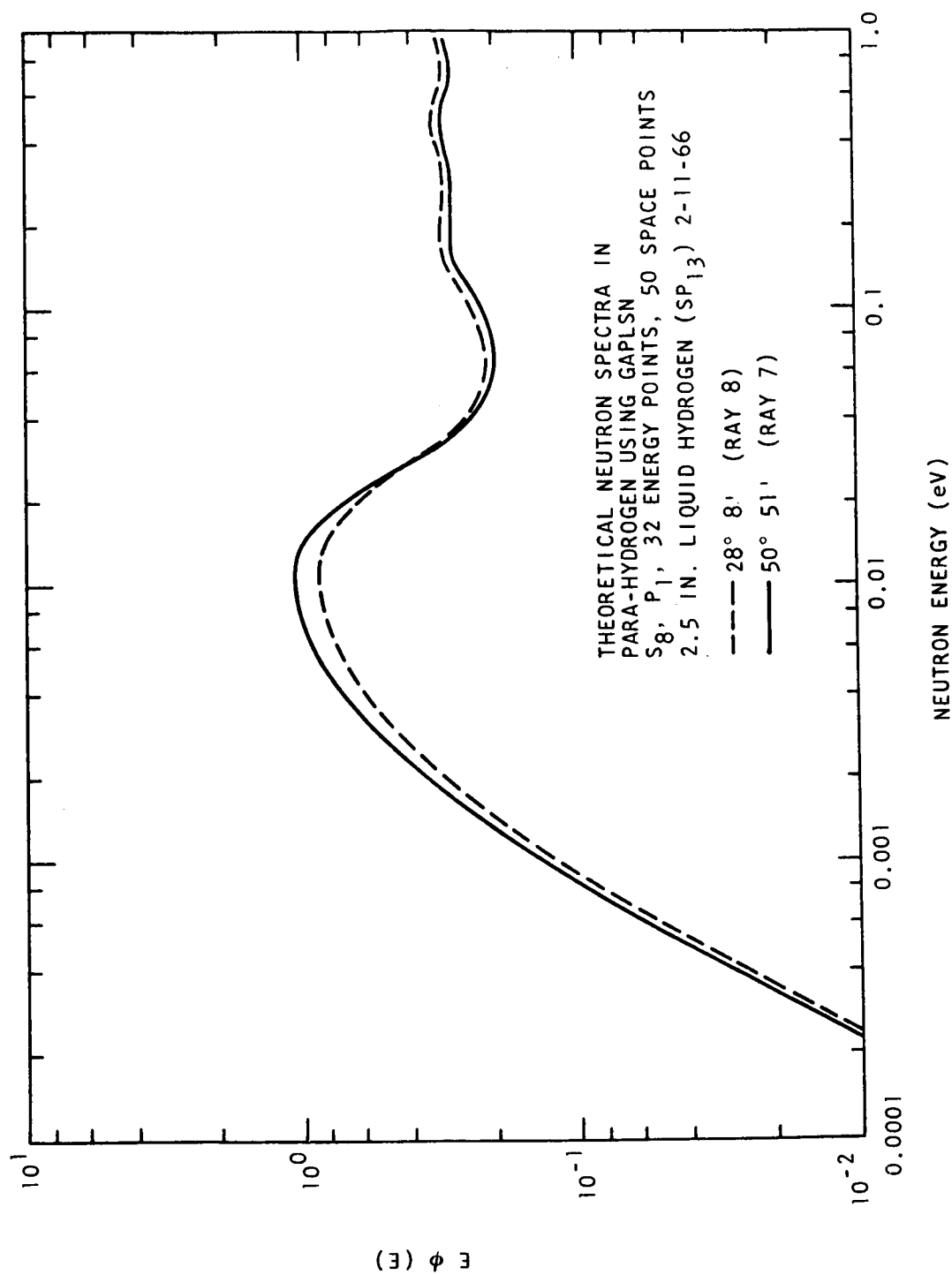


Fig. 18--S<sub>8</sub> calculation of the thermal neutron spectra for  
 2.5 in. of liquid hydrogen at angles of 28°8' and 50°51'

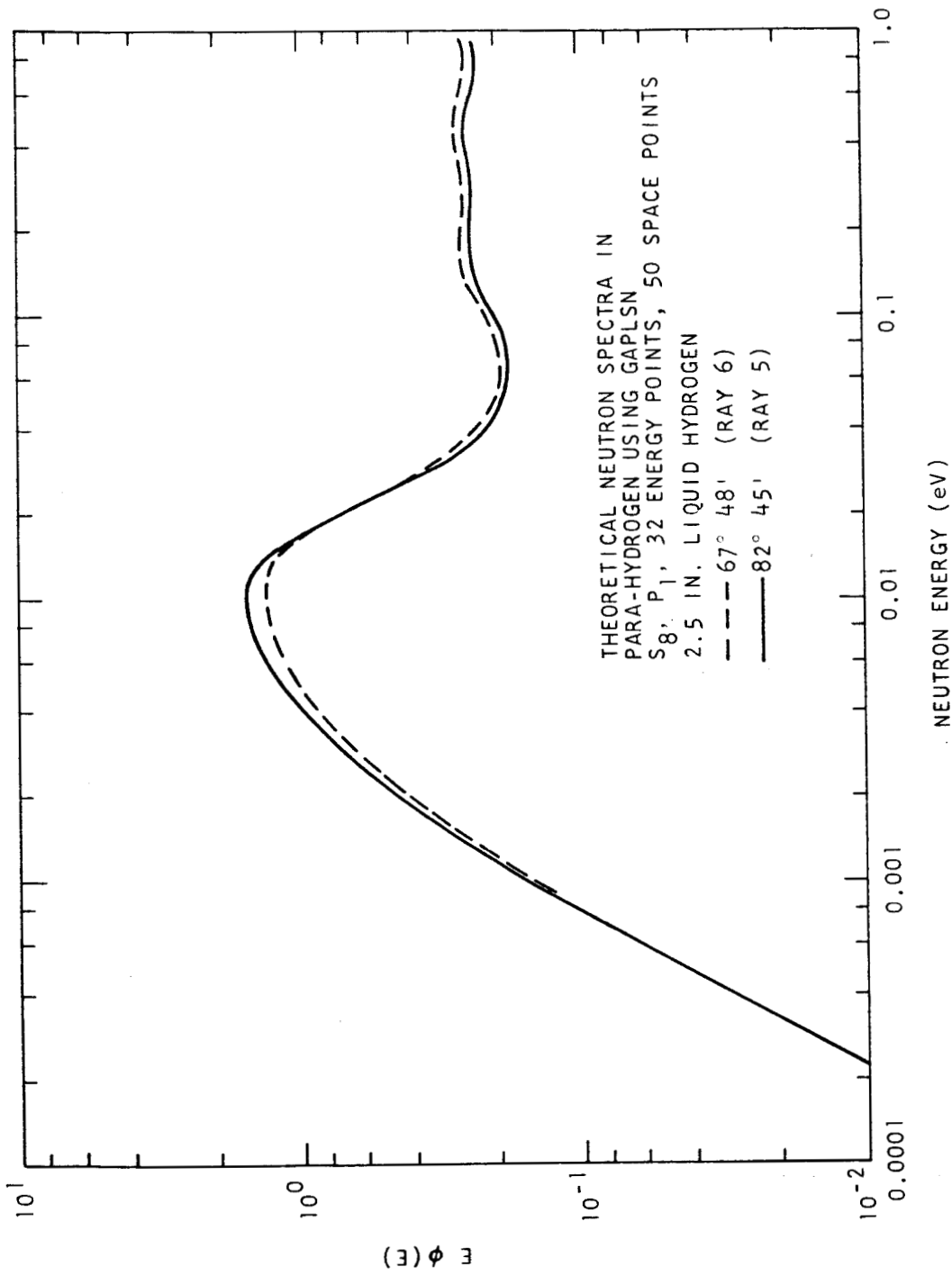


Fig. 19--S<sub>8</sub> calculation of the thermal neutron spectra for  
 2.5 in. of liquid hydrogen at angles of 67°48' and 82°45'

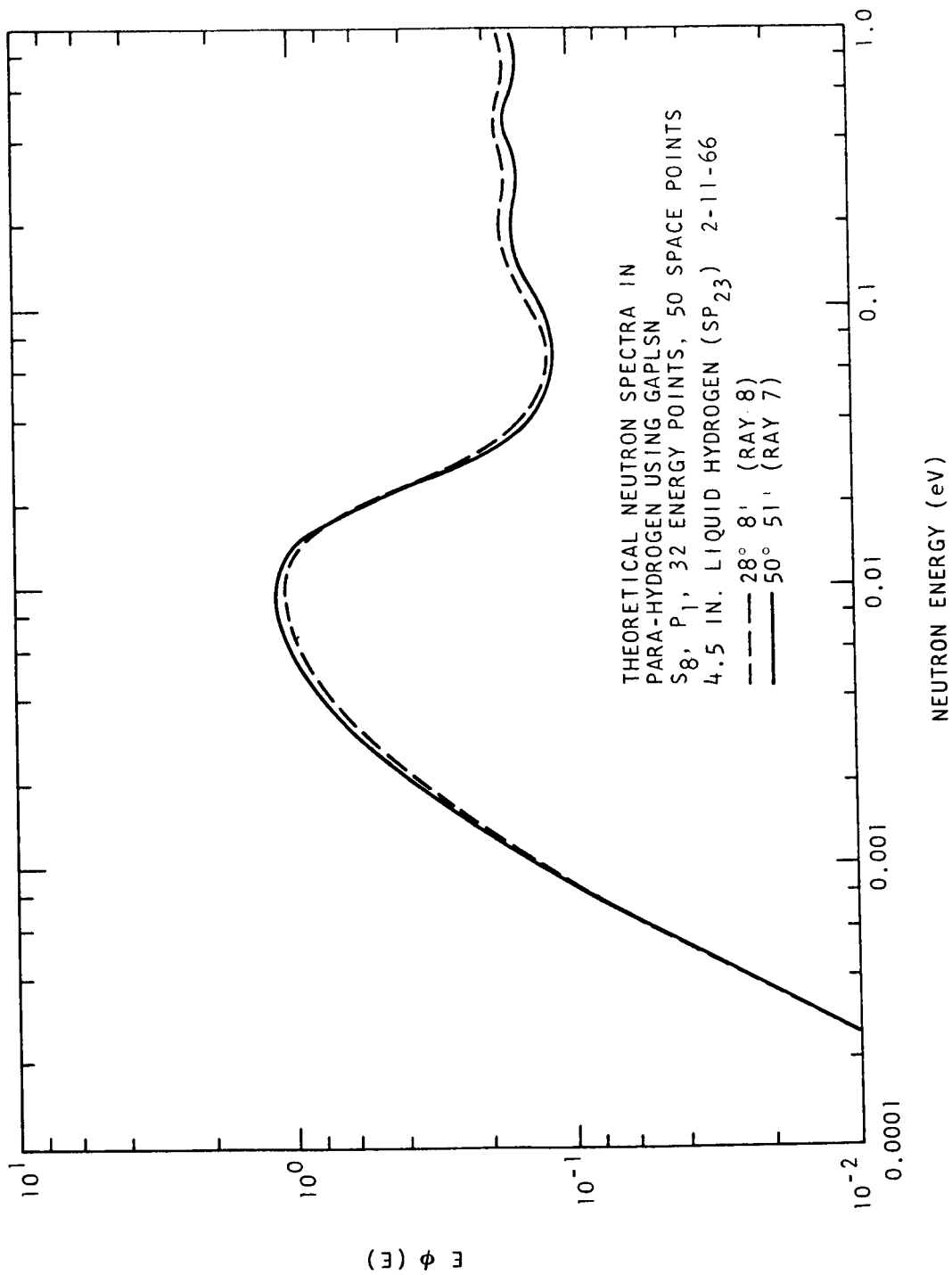


Fig. 20--S<sub>8</sub> calculation of the thermal neutron spectra for  
 4.5 in. of liquid hydrogen at angles of 28°8' and 50°51'

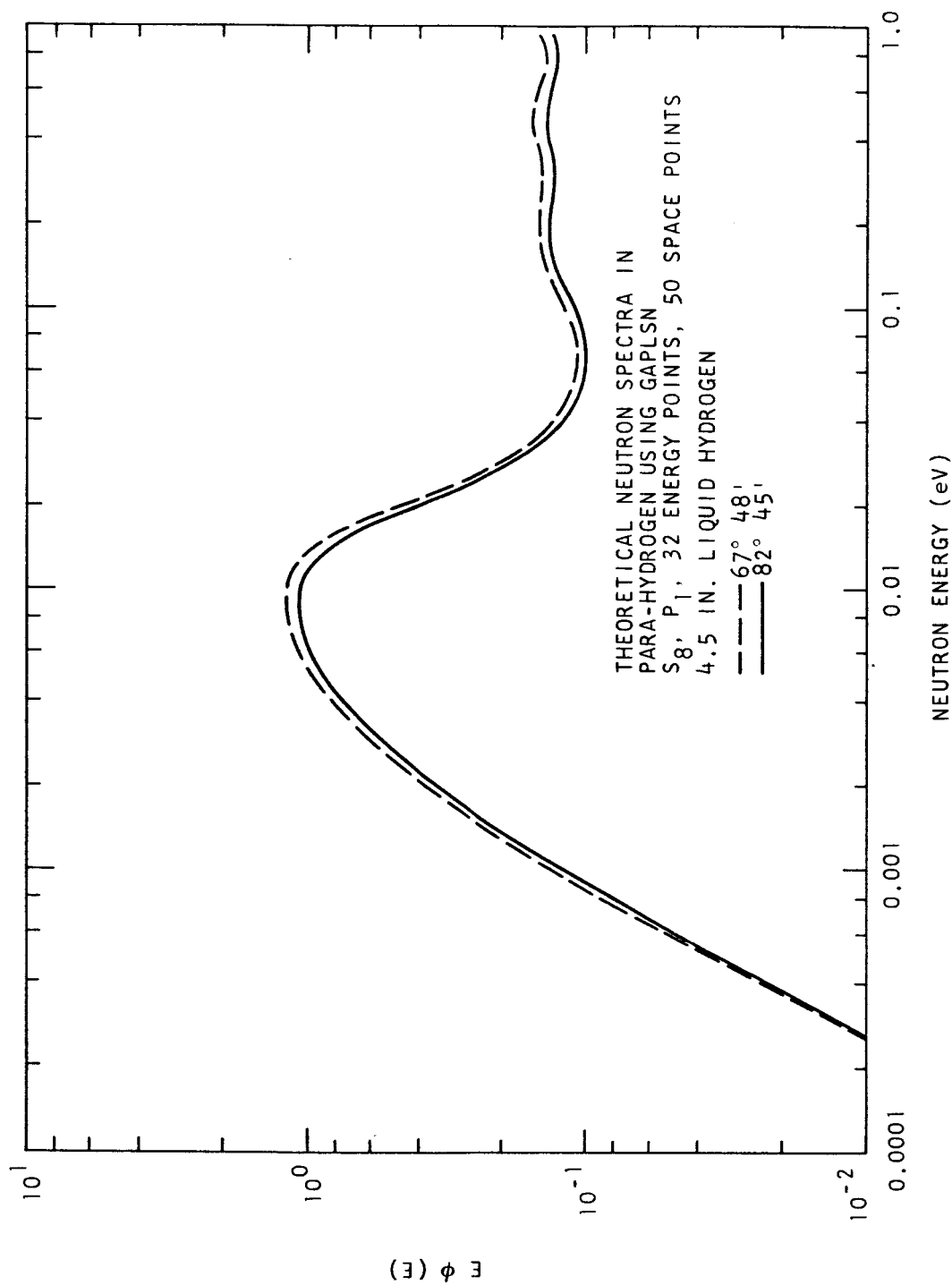


Fig. 21--S<sub>8</sub> calculation of the thermal neutron spectra for  
 4.5 in. of liquid hydrogen at angles of 67°48' and 82°45'

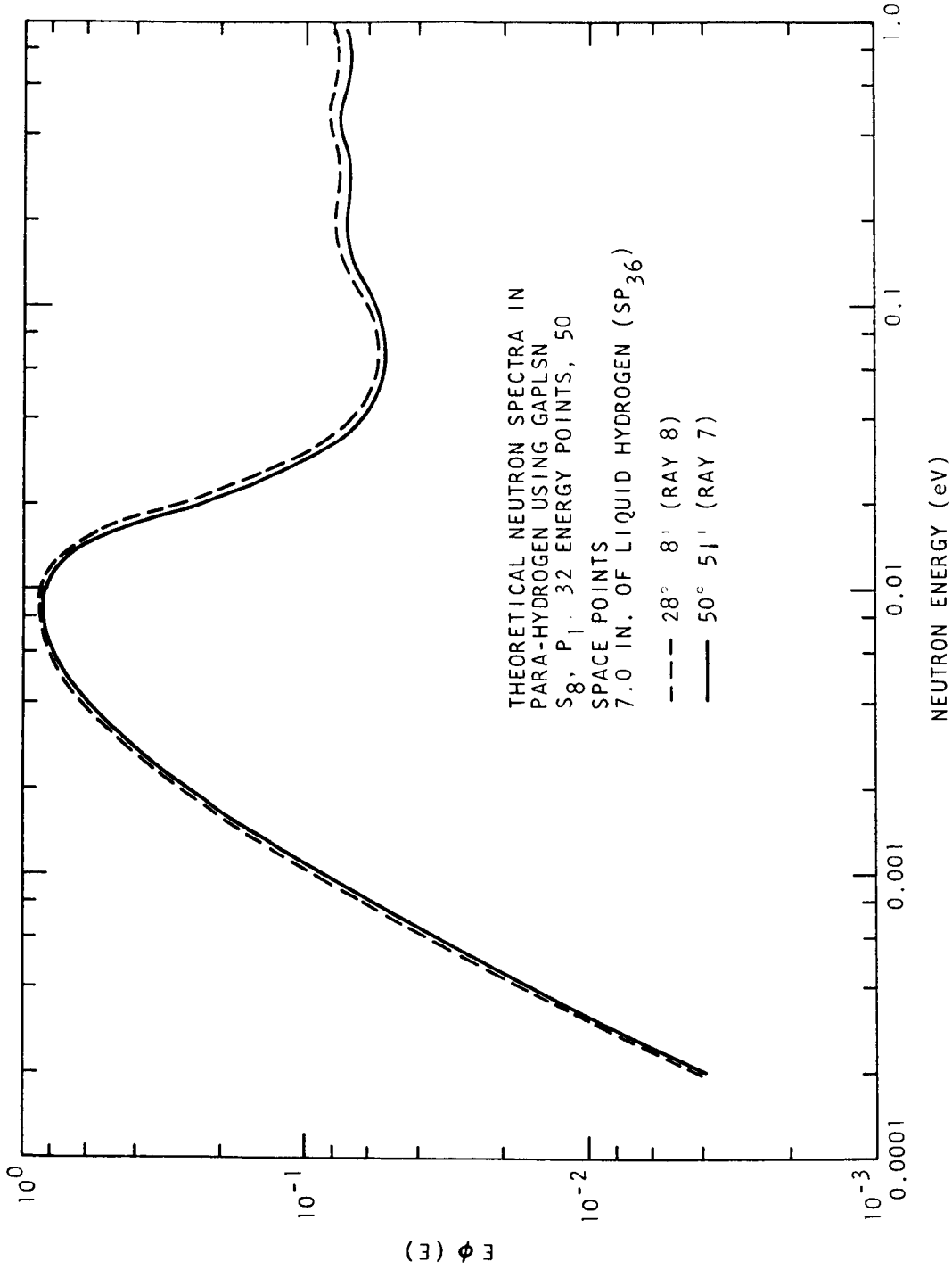


Fig. 22--S<sub>8</sub> calculation of the thermal neutron spectra for  
7.0 in. of liquid hydrogen at angles of 28°8' and 50°51'

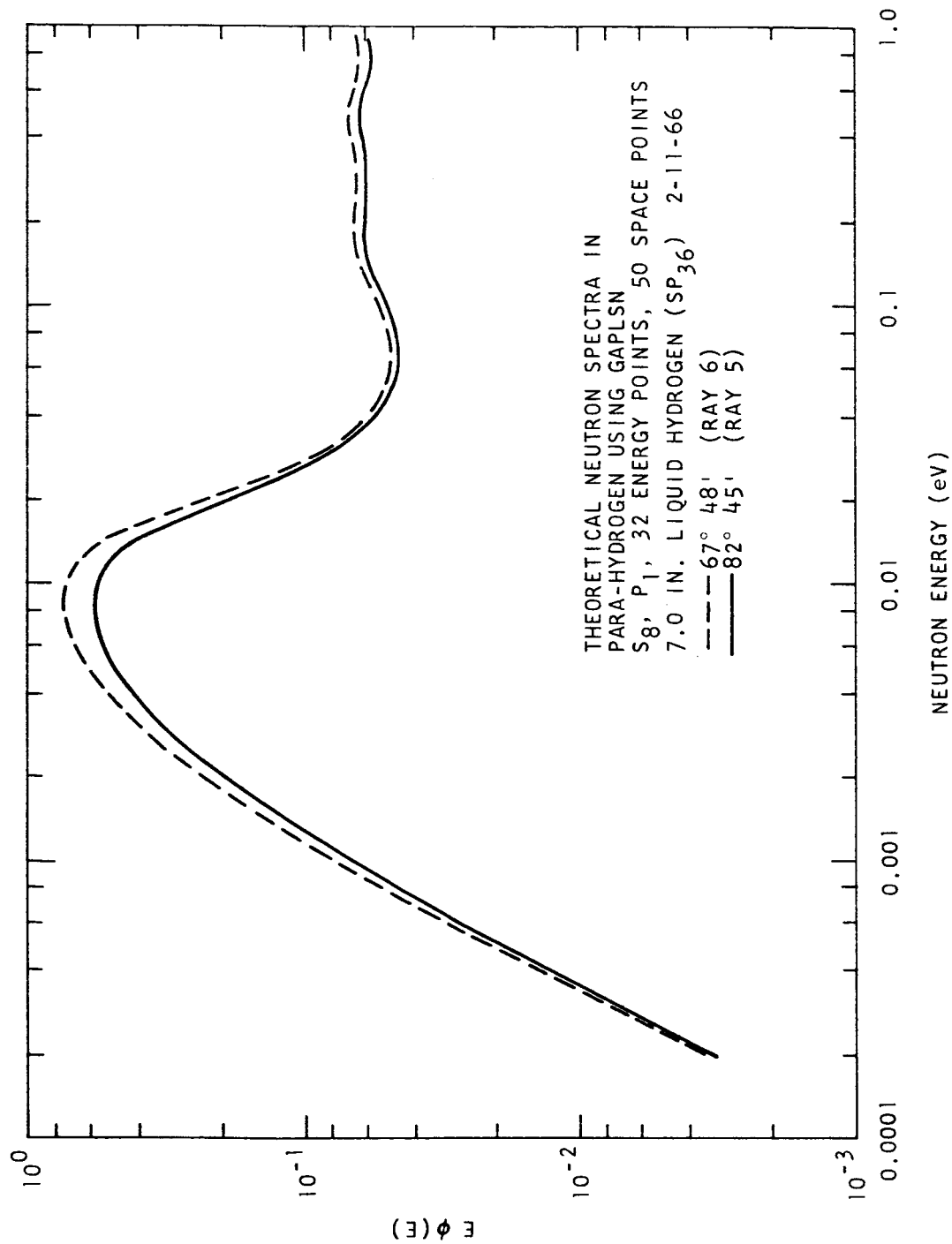


Fig. 23--S<sub>8</sub> calculation of the thermal neutron spectra for  
 7.0 in. of liquid hydrogen at angles of 67°48' and 82°45'

(0.5 MeV to 1 eV). These energy levels are presented in Table 2. Energy levels are shown for energies higher than 0.5 MeV since the problem must be calculated from the highest energy of the input source. On the basis of this approval calculations were then made in the intermediate neutron energy region, details of which are presented in the next section.

### 7.2.2 Details of the Calculations

The GAM-II code and the GAM-II library cross sections were used to obtain the 32 energy "broad-group" cross sections for the intermediate neutron spectrum calculations. The GAM-II library cross sections are tabulated for 99 fine-groups from 14.9 MeV to 0.41 eV and cross section matrices are included for  $P_0$  through  $P_3$  scattering in the laboratory system. The fine-group cross sections are derived from the basic pointwise data under the assumption that the intragroup flux is constant in lethargy ( $1/E$  in energy).<sup>(6)</sup> The GAM-II code requires a positive buckling, but since the buckling is negative it is better to use a small positive buckling since  $B \equiv 0$  gives only a  $P_0$  broad-group scattering matrix for use in GAPLSN. For this problem  $B$  was set equal to  $1 \times 10^{-5}$ .

The source spectrum for the GAM-II calculation was a U-235 fission source. The stainless steel of the baffles was homogenized with the liquid hydrogen. The reduced atom density for the liquid hydrogen was  $4.122 \times 10^{-2}$  atoms/barn-cm. The reduced atom density for the stainless steel was  $2.09 \times 10^{-3}$  atoms/barn-cm and is listed in the GAM-II library as tape nuclide number 202.

The source input to GAPLSN was calculated using the LAZYP code<sup>(6)</sup> which uses the measured fast neutron source spectrum as input. Source spectra are interpolated between measured points averaged over a group, and reduced to  $1/V$  neutrons/cm<sup>3</sup> sec (so that when multiplied by the volume  $V$  the source intensity is unity) by the LAZYP code.



Table 2  
 ENERGY LEVELS USED FOR  
 INTERMEDIATE NEUTRON ENERGY CALCULATIONS

<u>Group</u>	<u>Energy Level (eV)</u>
1	$1.492 \times 10^7$
2	$1.000 \times 10^7$
3	$7.408 \times 10^7$
4	$5.488 \times 10^6$
5	$4.065 \times 10^6$
6	$3.012 \times 10^6$
7	$2.019 \times 10^6$
8	$1.003 \times 10^6$
9	$7.427 \times 10^5$
10	$5.502 \times 10^5$
11	$3.337 \times 10^5$
12	$2.024 \times 10^5$
13	$1.111 \times 10^5$
14	$6.738 \times 10^4$
15	$4.087 \times 10^4$
16	$2.479 \times 10^4$
17	$1.503 \times 10^4$
18	$9.119 \times 10^3$
19	$5.531 \times 10^3$
20	$3.354 \times 10^3$
21	$2.035 \times 10^3$
22	$1.234 \times 10^3$
23	$7.485 \times 10^2$
24	$4.540 \times 10^2$
25	$2.754 \times 10^2$
26	$1.670 \times 10^2$
27	$1.013 \times 10^2$
28	$6.144 \times 10^1$
29	$2.260 \times 10^1$
30	$1.370 \times 10^1$
31	8.315
32	5.043

The source input to GAPLSN was a nearly normal source contained in the first ray or angular interval  $\mu = -1$  to  $\mu = .99999$ . Slab geometry was used for the GAPLSN calculation and the source was treated as an isotropic surface source. Therefore, in LAZYP the volume was taken as unity. The angular mesh boundaries (in  $\mu = \cos\theta$ ) for the GAPLSN slab calculation and the group surface source,  $Q_4$ , are given in Table 3. The source is assumed to be on the right hand side of the slab, so the angles of interest are negative  $\mu$ . A zero transverse buckling was used in these calculations. A variable angle,  $S_{16}$ , version of GAPLSN was used. To obtain the mean angles of 5, 15, 37, 53, 66, and 78°, two separate calculations were used for the  $S_{16}$  calculation since these angular regions of the mean angles overlapped. Mean angles of 5, 37, and 66° were obtained in one calculation and 15, 53, and 78° in the other. The calculations were done for a  $P_3$ , variable angle  $S_{16}$ , 60 space points with a spatial mesh of 0.65 cm and a 32 energy group. This spatial mesh provided a backscattering thickness of 6 cm and used the memory capacity of the IBM 7044. The data are presented in graphical form for the five thicknesses in Figs. 24, 25, 26, 27, and 28. The fast neutron energy region is shown since the problem must be calculated from the highest energy of the input source.

## 8. NEUTRON SPECTRUM MEASUREMENTS BY TIME-OF-FLIGHT TECHNIQUES

### 8.1 Thermal Neutron Spectrum Measurements

Under the present contract the neutron spectra for all experiments performed must be calculated. As was noted in Section 7, we could not calculate anything greater than an  $S_4$ ,  $P_1$ , 32 energy groups for a thickness of 13 inches. The mean angles for this calculation were 39°14' and 75°31'. Since we were physically limited to measurements between 0 and

Table 3  
SLAB, VARIABLE ANGLE GAPLSN

$\mu$  bounds for 5, 37, and 66° calculation 3-5-66

-1.0000	-0.99999	0.000	0.125
-0.99999	-0.99240	0.125	0.250
-0.99240	-0.89661	0.250	0.375
-0.89661	-0.70066	0.375	0.500
-0.70066	-0.50471	0.500	0.625
-0.50471	-0.30876	0.625	0.750
-0.30876	-0.18043	0.750	0.875
-0.18043	0.00000	0.875	1.000

$\mu$  bounds for 15, 53, 78° calculation 3-7-66

-1.0000	-0.99999	0.000	0.125
-0.99999	-0.99239	0.125	0.250
-0.99239	-0.93947	0.250	0.375
-0.93947	-0.70066	0.375	0.500
-0.70066	-0.50297	0.500	0.625
-0.50297	-0.30876	0.625	0.750
-0.30876	-0.10705	0.750	0.875
-0.10705	0.00000	0.875	1.000

<u>Group</u>	<u><math>Q_4</math></u>
1	$5.4678 \times 10^2$
2	$1.8022 \times 10^3$
3	$4.2419 \times 10^3$
4	$6.6776 \times 10^3$
5	$9.2173 \times 10^3$
6	$1.6162 \times 10^4$
7	$3.9795 \times 10^4$
8	$2.3523 \times 10^4$
9	$2.3028 \times 10^4$
10	$3.0221 \times 10^4$
11	$1.9219 \times 10^4$
12	$1.4249 \times 10^4$
13	$6.9370 \times 10^3$
14	$4.3629 \times 10^3$

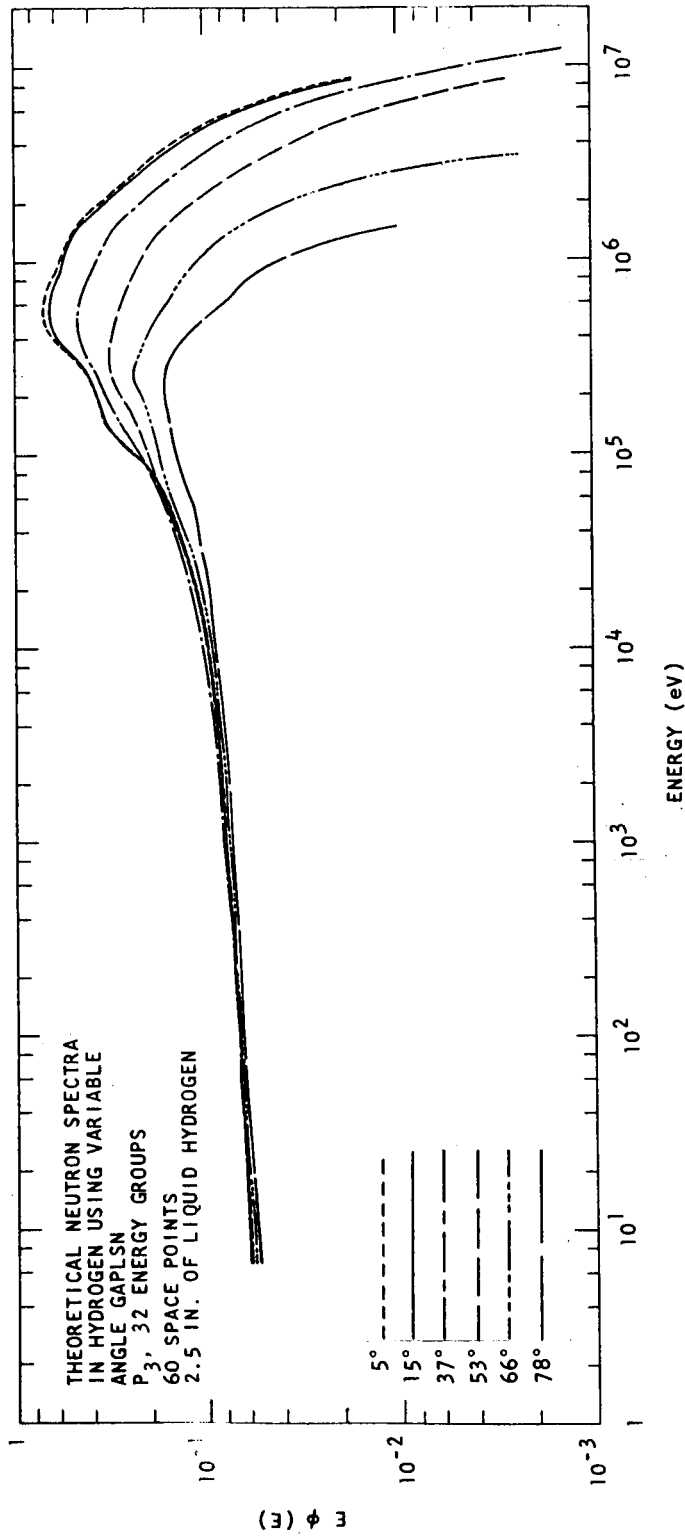


Fig. 24--Intermediate neutron spectrum calculations  
for 2.5 in. of liquid hydrogen

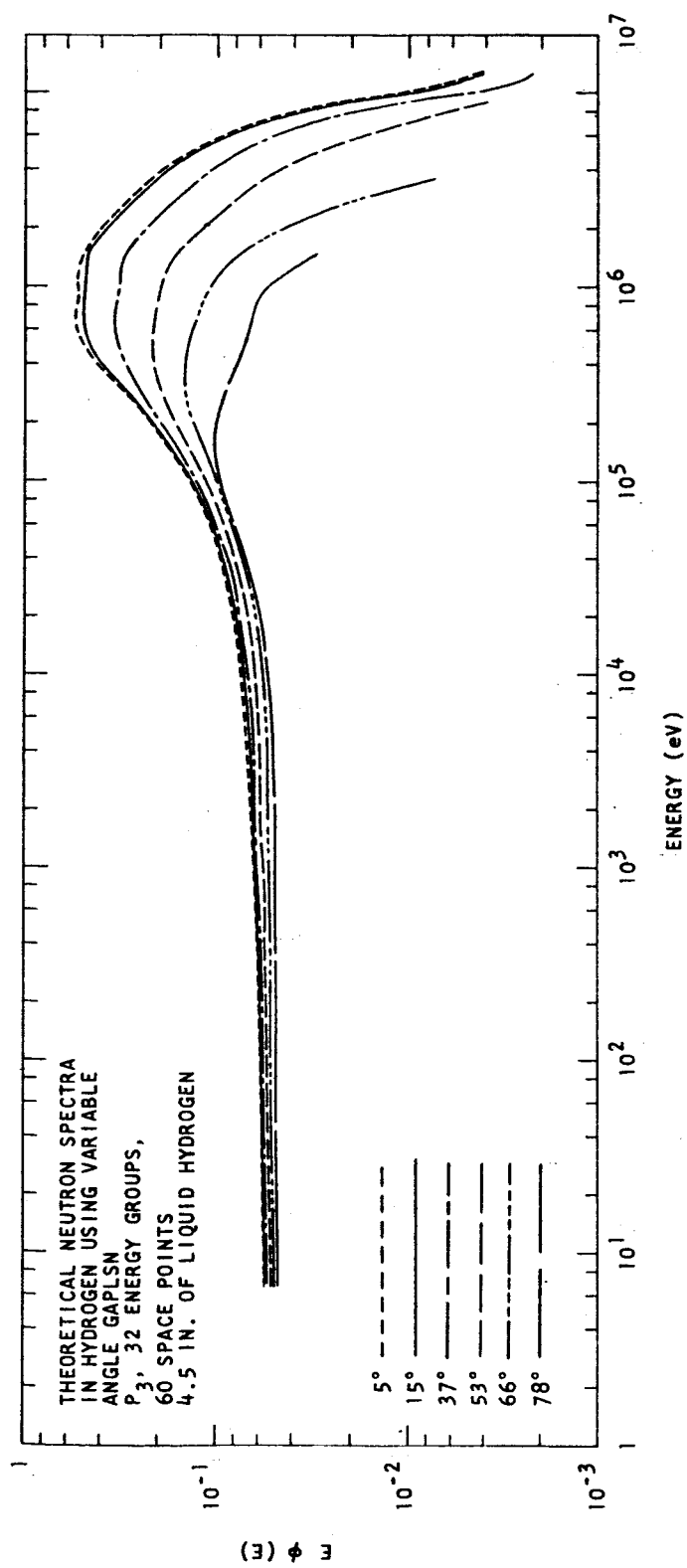


Fig. 25--Intermediate neutron spectrum calculations  
for 4.5 in. of liquid hydrogen

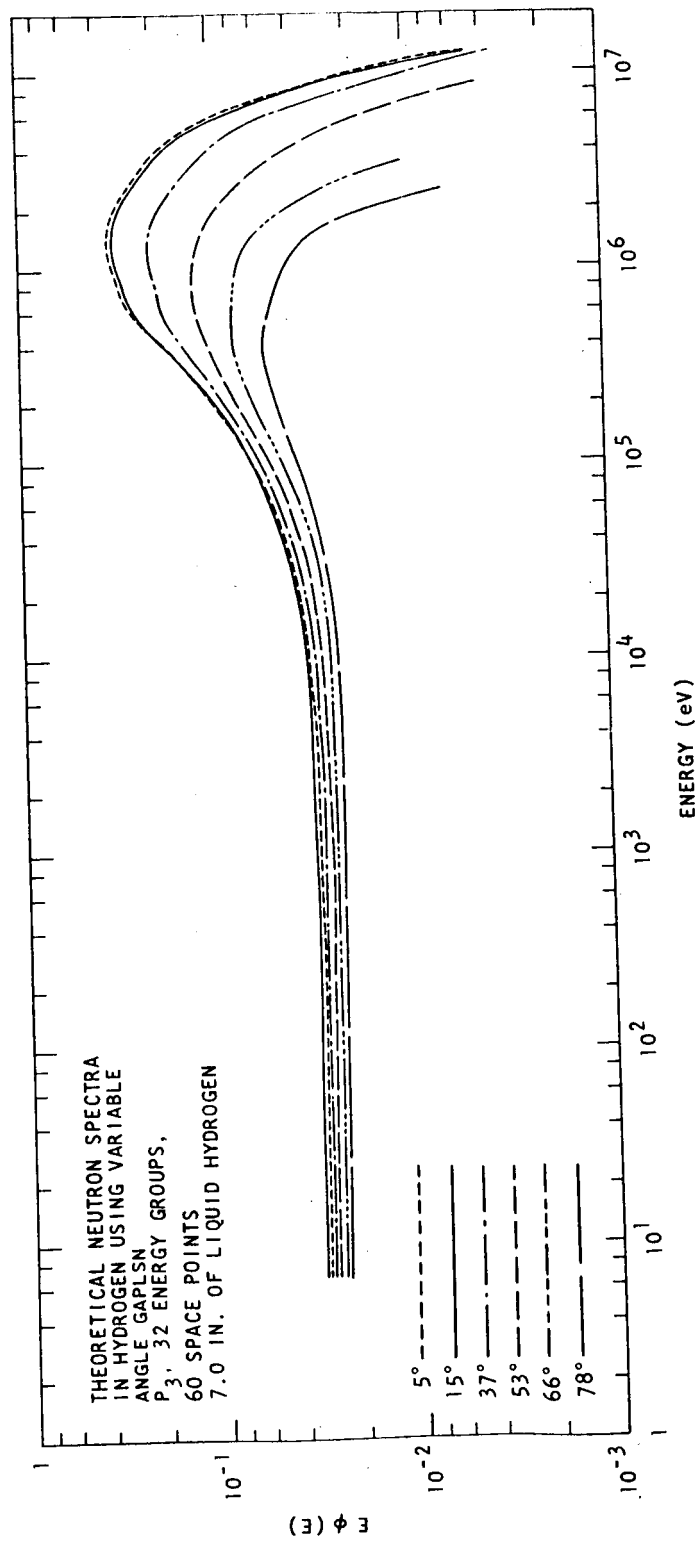


Fig. 26--Intermediate neutron spectrum calculations  
for 7.0 in. of liquid hydrogen

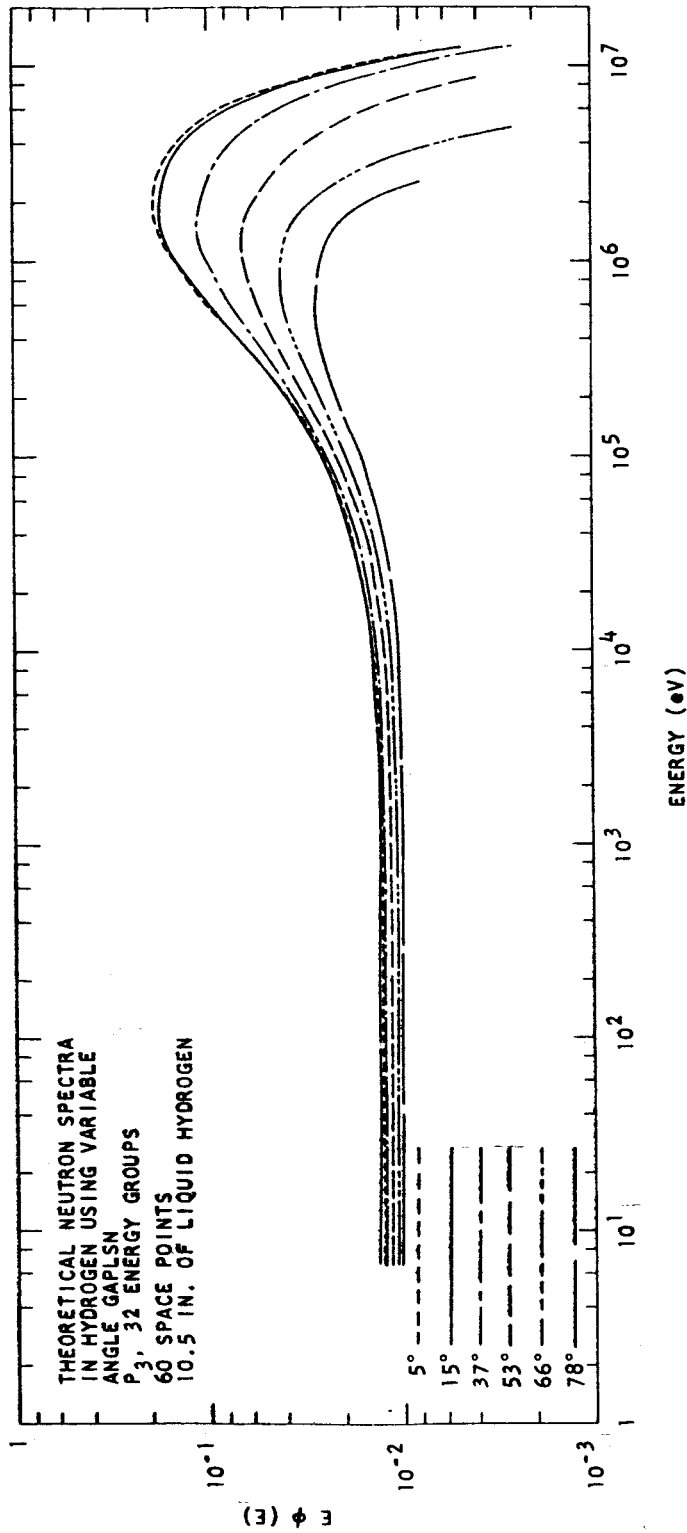


Fig. 27--Intermediate neutron spectrum calculations  
for 10.5 in. of liquid hydrogen

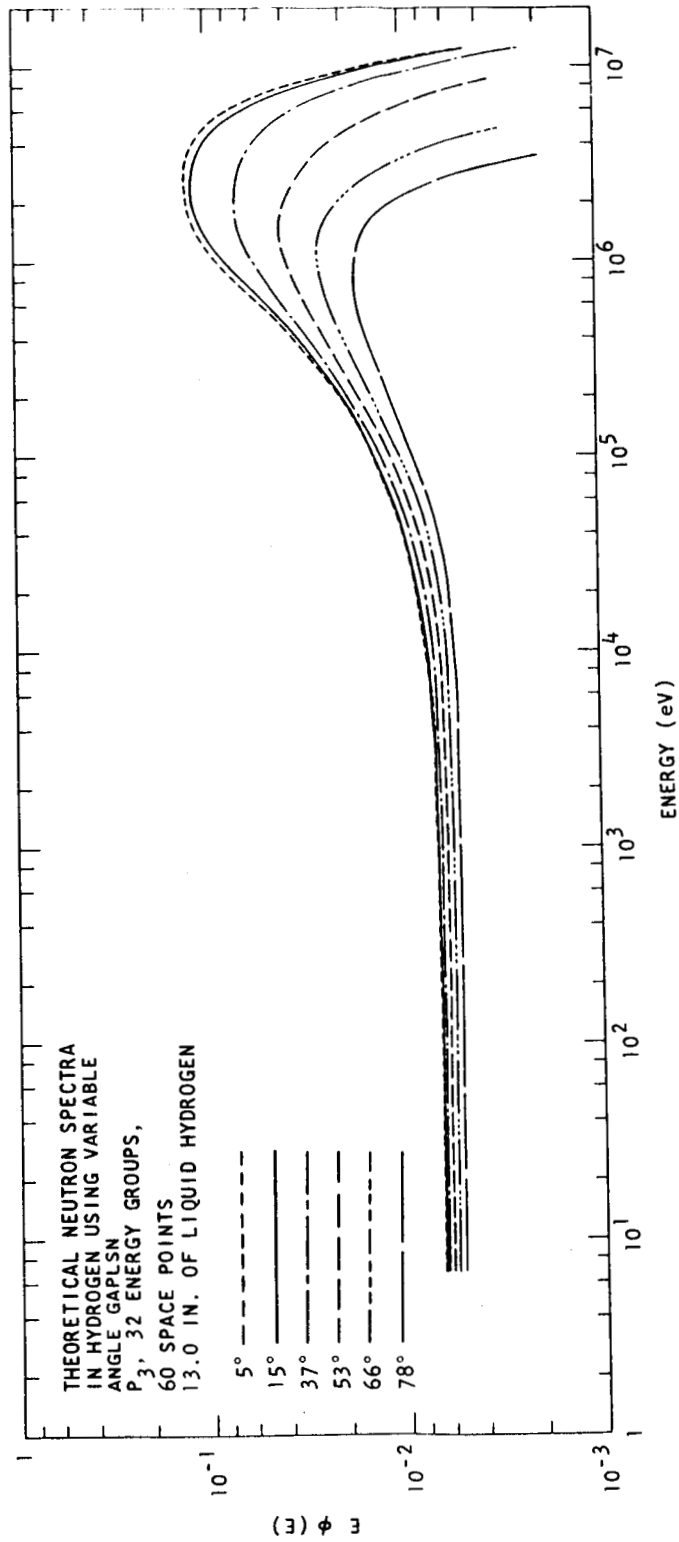


Fig. 28--Intermediate neutron spectrum calculations  
for 13.0 in. of liquid hydrogen



$90^{\circ}$  and we were required to make measurements at two angles, it was recommended to the Project Manager that measurements of thermal neutron spectra be made at  $39^{\circ}$  and  $75^{\circ}$  for the 2.5, 4.5, 7.0, 10.5, and 13.0 in. thicknesses of liquid hydrogen. These recommended angles were approved by the Project Manager.

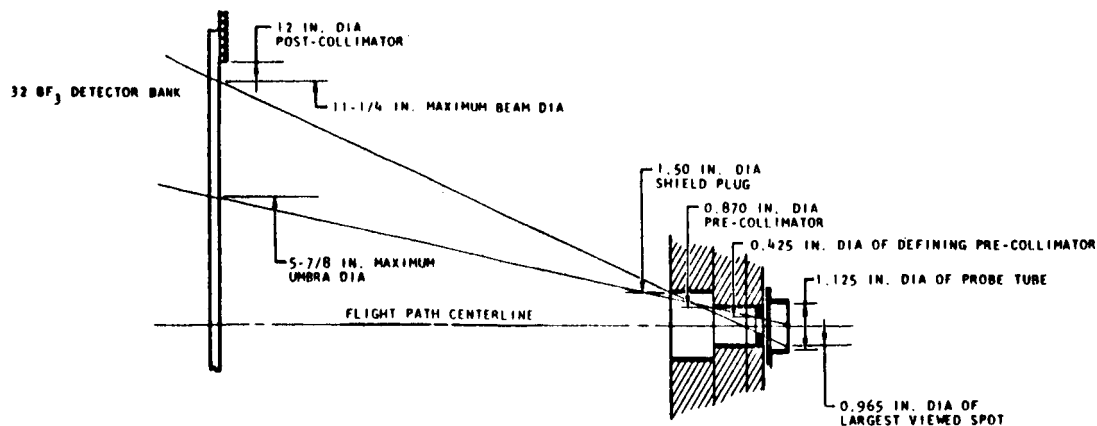
The thermal neutron angular spectra were measured by extracting a collimated beam from the  $\text{LH}_2$  cryostat and measuring the time of flight over 16 meters. Time-zero was defined by turning on the analyzer sweep of the TMC 1024-channel analyzer with a Model 212 time-of-flight logic unit with an electrical pulse from the Linac injector trigger, which has a fixed relationship with the electron current pulse. A channel width of 40  $\mu\text{sec}$  was used in these experiments.

The collimator viewed a spot at the inner end of the 21 in. long probe tube through two thin stainless steel windows. The probe tube was filled with 5 psig of helium and was located at the center of the hemispherical section of the cryostat. The collimating system is shown in Fig. 29. The thermal neutron precollimator made of boron nitride 0.425 in. in diameter and 8.0 in. long was fitted into the 0.870 in. i.d. precollimator of the fast neutron flight path system. A post-collimator was placed immediately adjacent to the detector bank; this collimation system gave a viewed spot size on the inner probe tube window of 1.00 in. This allowed a misalignment tolerance of 0.125 in. which was well within our alignment capability. The probe tube was aligned with the flight path system as explained in Section 5. The background plug, described in Section 6 was attached to the precollimator end of the flight path and was moved in and out of the flight path by a remote cable system. The pressure in the 16-meter flight path was 145 microns.

The thermal neutron detector was an array of 32  $\text{BF}_3$  counters with their symmetrical axis perpendicular to the flight path direction and stacked in a 6, 7, 6, 7, 6 order. The  $\text{BF}_3$  detector bank was housed

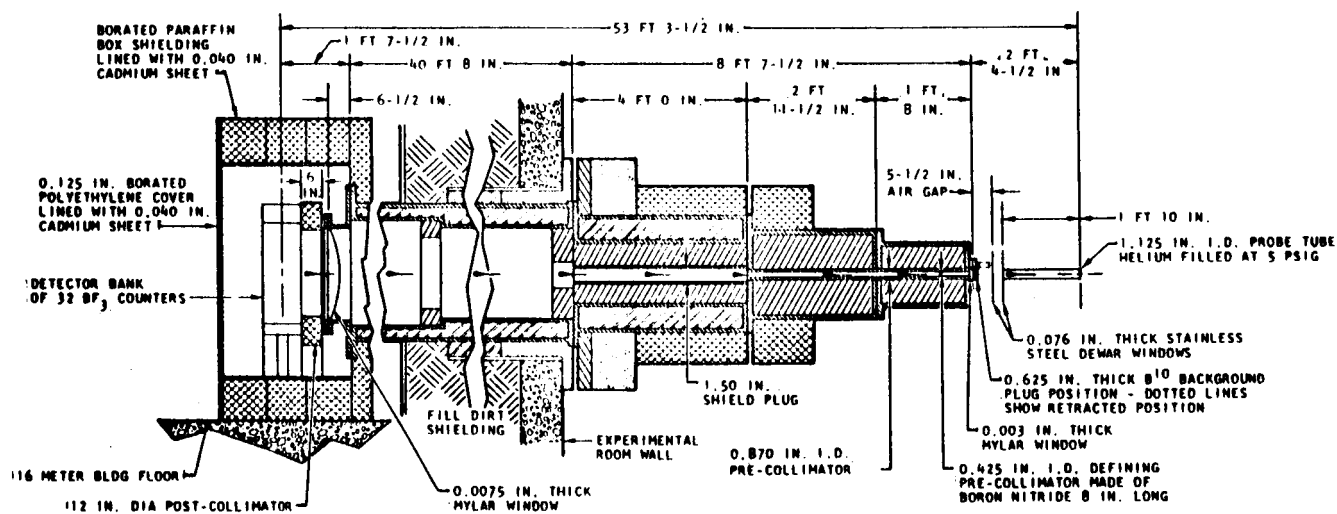
## RAY DIAGRAM

VERTICAL SCALE IS 48 X HORIZONTAL SCALE



## FLIGHT PATH CROSS SECTION

HORIZONTAL SCALE IS ONE-HALF VERTICAL SCALE



## MATERIAL CODE

	LEAD		STEEL-ALUMINUM		DIRT
	BORIC ACID		HIGH-DENSITY (MAGNETITE) CONCRETE		NORMAL CONCRETE
	LEAD AND BORIC ACID IN EPOXY MIXTURE		BORIC ACID IN PARAFFIN MIXTURE		

Fig. 29--Flight path configuration for thermal neutron experiments

in a small low-background building made from 12 by 12 by 6 in. wooden boxes filled with hydrous boric acid. The inner walls of this housing were lined with 25 wt % borated polyethylene to absorb scattered thermal neutrons.

The  $\text{LH}_2$  cryostat was covered with 0.030 in. of cadmium (see Fig. 30) to prevent the influence of thermal neutron room return.

Electrons from the Linear Accelerator impinge on the cylindrical surface of the water-cooled uranium source and generate bremsstrahlung, which in turn produce a spectrum of fast neutrons via the  $(\gamma, n)$  and  $(\gamma, \text{fission})$  reactions. The  $\text{LH}_2$  cryostat is fixed for a particular angle and filled to the largest thickness with  $\text{LH}_2$ . The angular neutron spectrum measurements proceed from the largest thickness. For each thickness signal and background measurements were made and the fast neutron source intensity monitored for each. The uranium source and source support, beam tube guide, aluminum slug monitor and holder, and mirror used for monitoring the electron beam are shown in Figs. 31 and 32.

## 8.2 Fast Neutron Spectrum Measurements

The purpose of these measurements was to recheck some of the fast neutron spectrum measurements performed in the previous program, establish whether experimental conditions were the same for the present measurements, and insure that all possible corrections to the previous data had been accomplished. It was recommended that fast neutron spectrum measurements be repeated at  $0^\circ$  as a function of hydrogen thickness and at a larger angle,  $37^\circ$ , for various thicknesses but generally at the greater thicknesses. These measurements were to be limited to about five runs but not to exceed 20 hours of Linac operation since we are contractually limited to this number of machine hours. A depleted uranium filter 3.144 cm thick would be used to suppress the gamma-ray background for these measurements; this filter was not used on the previous program. These recommendations were approved by the Project Manager.

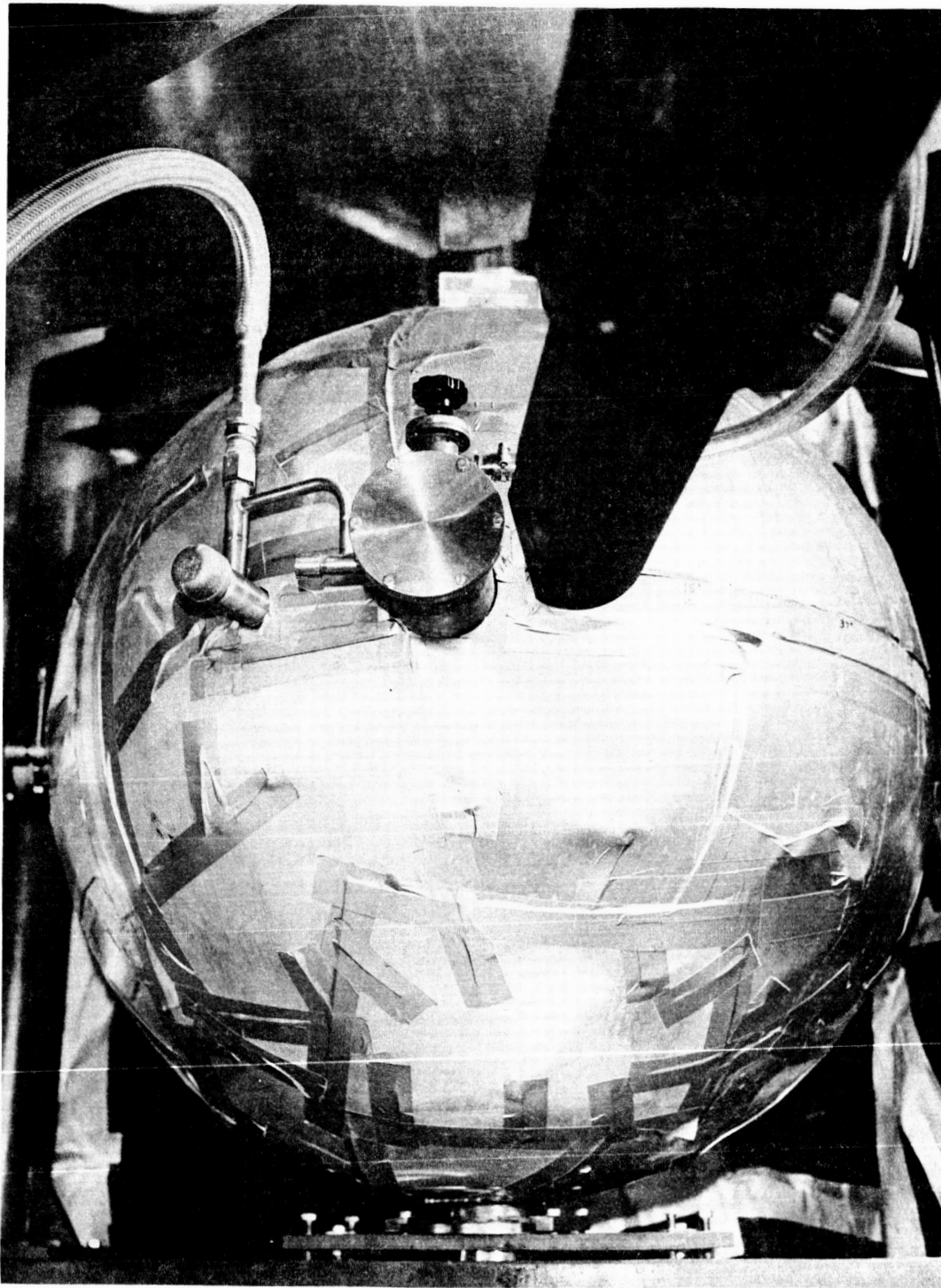


Fig. 30--LH<sub>2</sub> cryostat showing cadmium covering

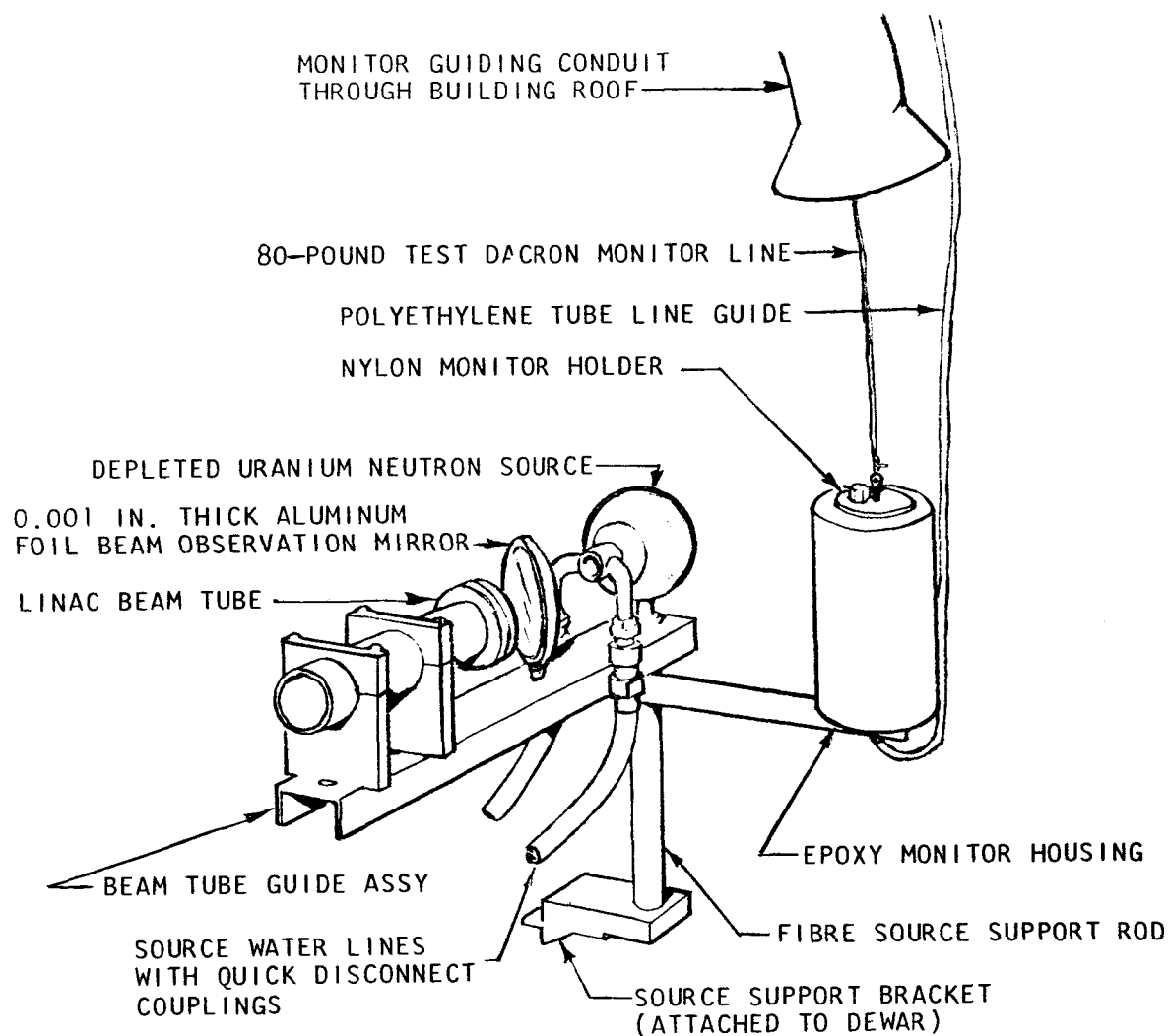


Fig. 31--Uranium source and support, beam tube guide, aluminum slug monitor and holder, and mirror used for monitoring electron beam

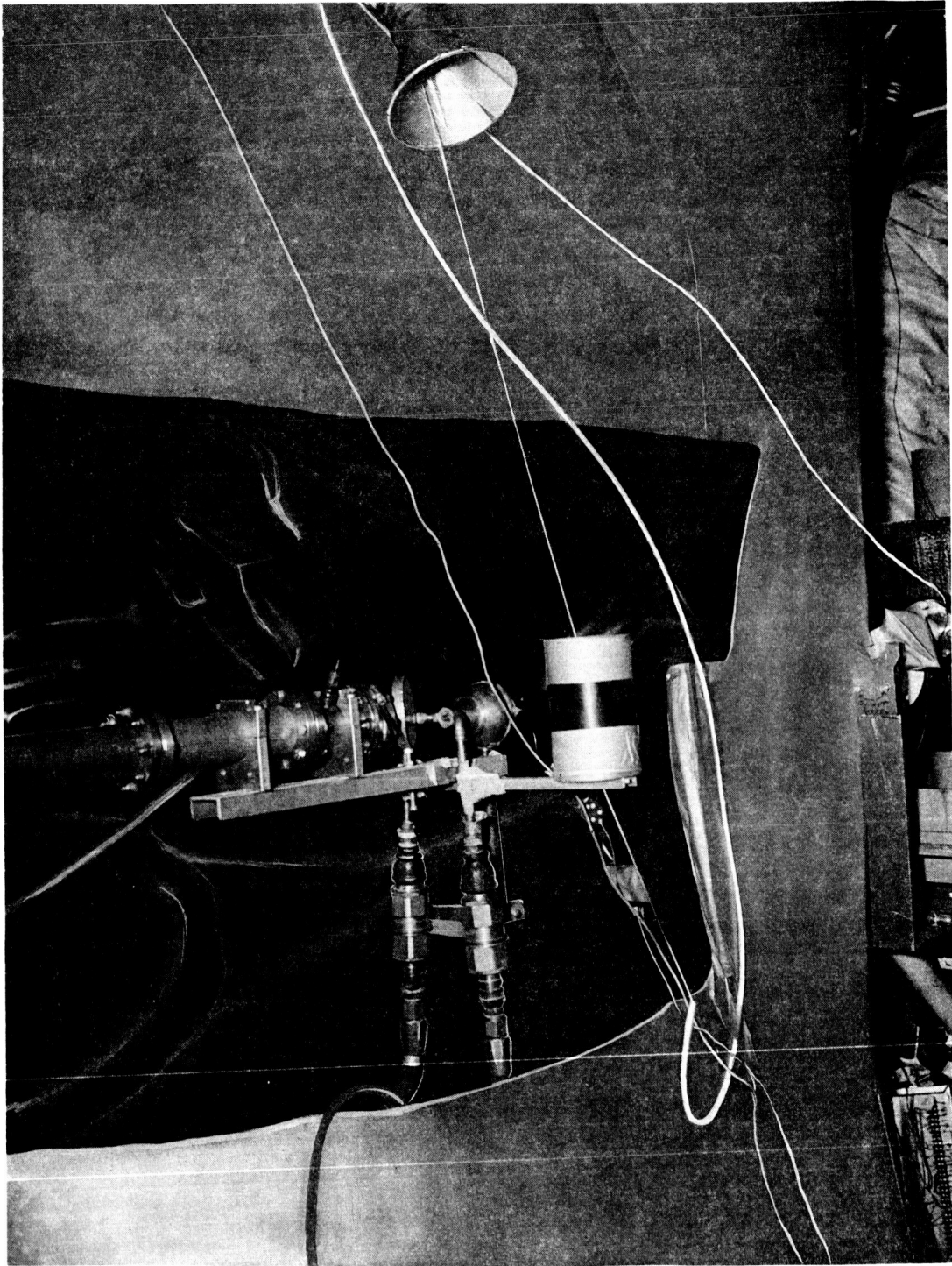


Fig. 32--Photograph of uranium source

The ambient background composed primarily of the natural radioactivity of the liquid scintillator and environment and cosmic radiation was reduced by shielding the detectors in a dolly-mounted lead "housing" around the entire detector system, open at both ends to allow the highly collimated neutron beam to pass through without striking the walls of the "housing." The walls were 2-in. thick lead and the "housing" was 40 in. long.

Fast neutron spectrum measurements were performed at thicknesses of 13.0, 7.0, and 2.5 in. of  $\text{LH}_2$  and the empty dewar for  $0^\circ$ , and thicknesses of 10.5, 4.5, and 2.5 in. of  $\text{LH}_2$  and the empty dewar for  $37^\circ$ .

The windows of the flight path system were mylar, while on the previous program they were aluminum. This allowed transit alignment of the probe tube of the  $\text{LH}_2$  cryostat and the fast neutron detectors without the necessity of breaking the vacuum in the flight path. Details of the 50-meter flight path collimation system are shown in Fig. 33. The large diameter steel drift tubes are evacuated to rough vacuum by mechanical forepumps. The collimation system is designed so that the edge of the precollimator nearest the experimental assembly and the 3.0 in. i.d. steel collimator at the 16-meter position define the viewed spot size at the assembly and the beam spot size at the detector. With a given dewar probe tube inner diameter of 1.125 in. at 28 in. from the precollimator, an 0.870 in. i.d. precollimator gave a viewed spot diameter on the probe tube inner window of about 1.03 in.; this allowed a misalignment tolerance of 0.095 in., which was well within our alignment capability. The maximum beam spot size at the 50-meter detector position produced by this collimation system was 10.62 in. One additional post-collimator was added at the 32-meter position to eliminate stray background-producing gamma rays and high energy neutrons from reaching the detector. A depleted uranium plate 30.5 by 30.5 by 3.144 cm thick at the 16-meter position suppresses bremsstrahlung flash and any delayed gamma rays from the fast neutron source or the  $\text{LH}_2$  cryostat.

VERTICAL SCALE IS 64 X HORIZONTAL SCALE



The angular neutron spectra were measured by the time-of-flight method over a distance of 50 meters. The time delay between the production and detection was measured electronically by using the TMC 1024-channel analyzer with a Model 201 time-of-flight logic unit. The analyzer sweep was started with the Linac injector trigger, stopped by a detector pulse above a certain discriminator threshold or bias, and stored in the proper time channel.

The detectors were proton-recoil liquid scintillation counters. Two detectors were used in the experiments; one was a 2-in. diameter by 2.5-in. long cylinder of NE-211 liquid scintillator, mounted with the neutrons incident perpendicular to the symmetry axis and the second detector was a 5 in. by 5 in. NE-211 liquid scintillator with neutrons incident parallel to the symmetry axis. Both of these detectors were biased at the peak of the total absorption peak of the 60 keV  $\text{Am}^{241}$  gamma ray.

The depleted uranium fast neutron source and monitoring method were the same as for the thermal neutron spectrum measurements. The 0.030-in. cadmium covering on the  $\text{LH}_2$  cryostat remained the same as for the thermal neutron measurements.

### 8.3 Intermediate Neutron Spectrum Measurements

The intermediate neutron spectrum measurements began on March 16, 1966. Since the bulk of these measurements will be performed during the next report period, a discussion of the intermediate neutron spectrum measurements will be included in the next report.

## 9. WORK PLANNED FOR NEXT REPORT PERIOD

The bulk of the work planned for the next report period will consist in reducing the data of the angular spectral measurements made to date in the fast, intermediate and thermal neutron region.

The majority of the intermediate neutron spectrum measurements will be made during this period.

Reduction of the data will include modification of the efficiency of the detectors for the transmission of the flight path. Processing of the large number of experimental runs will be accomplished by using the General Atomic computer code ECTOPLASM. Essentially, this code converts the raw data or time spectrum,  $N(t)$ , into an energy spectrum,  $N(E)$ , after corrections are applied for background, normalization, dead-time losses, and detector efficiency.

## REFERENCES

1. Y. D. Naliboff, "LHK - An IBM 7044 Code to Calculate Cross Sections and Kernels for Liquid Para- and Ortho-Hydrogen, " NASA Report NASA-CR-54227, General Atomic Division, General Dynamics Corporation, July 1964.
2. J. A. Alexander, G. W. Hinman and J. K. Triplett, "GAPLSN - A Modified DSN Program for the Solution of the One-Dimensional Anisotropic Transport Equation, " General Atomic Report GA-4972 (1964).
3. H. A. Vieweg, G. D. Joanou and C. V. Smith, "GATHER-II - An IBM 7090 FORTRAN-II Program for the Computation of Thermal Neutron Spectra and Associated Multigroup Cross Sections, " General Atomic Report GA-4132, July 1963.
4. R. W. Vance and W. M. Duke, Applied Cryogenic Engineering, John Wiley and Sons, Inc., New York, 1962, p-38.
5. J. R. Beyster, et al., "Integral Neutron Thermalization Annual Summary Report, Oct. 1, 1961 through Sept. 31, 1962, " USAEC Report GA-3542, General Atomic Division, General Dynamics Corporation (1962).
6. A. E. Profio, "Verification of Analytical Techniques (GAPLSN - Transport Theory and O5R - Monte Carlo Theory) by Utilization of Measured Fast Neutron Spectra in Infinite Paraffin and Spherical Paraffin Shields, " Air Force Weapons Laboratory Report AFWL-TR-65-193, General Atomic Division, General Dynamics Corporation, March 1966.